Chapter 1

Introduction and Literature Review

Chapter 1

Introduction and Literature Review

1.1 Introduction

Today in the 21st century, energy is certainly one of the most critical and pressing issues on the global stage. The modern society has experienced massive increase in the global energy consumption due to the rapid growth of industrialization and human population. In the current age, fossil fuels are the most important source of energy. More than 70% of the energy consumption has been supplied by generating energy from traditional fossil fuels, e.g., oil, natural gas, and coal [1-3]. In 2022, 82% of the world total primary energy consumption was supplied by fossil fuels, including 26.7% of coal, 31.6% of oil, and 23.5% of natural gas, respectively (**Figure 1.1**) [4]. Moreover, forecasts made predictions that the global energy demand is set to grow by more than 25% to 2040 (International Energy Agency, 2018).

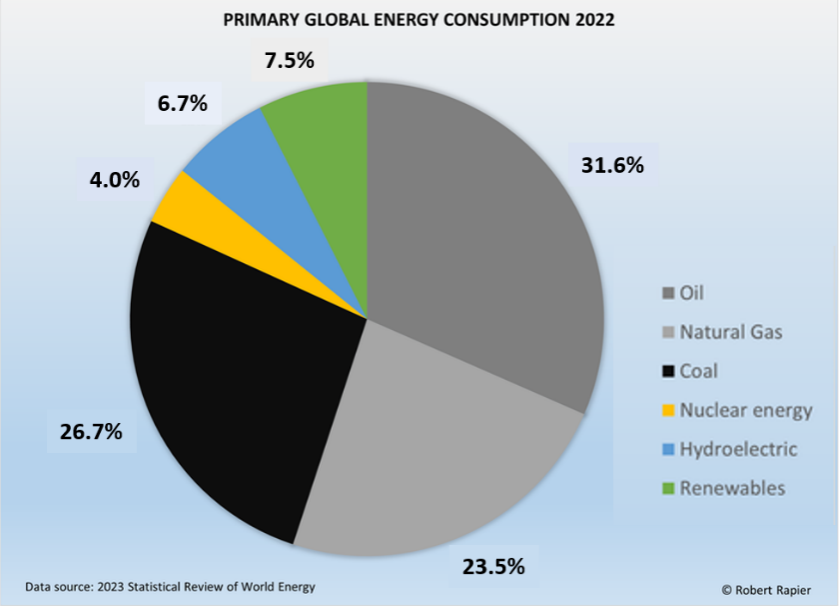

Figure 1.1 The world total primary energy consumption by fuels in 2022 [4].

Despite primary energy source, the fossil fuel combustion also generates a range of harmful pollutants such as CO_2, NO_x, and SO_x as byproducts. The overconsumption of fossil fuel causes

serious environmental issues such as global warming and atmospheric pollution that can eventually affect our lives. According to worldwide data, the electricity, heat, and transportation sectors are the major sources of CO_2 emissions, and it is expected to continue increasing in the future (**Figure 1.2**) [5].

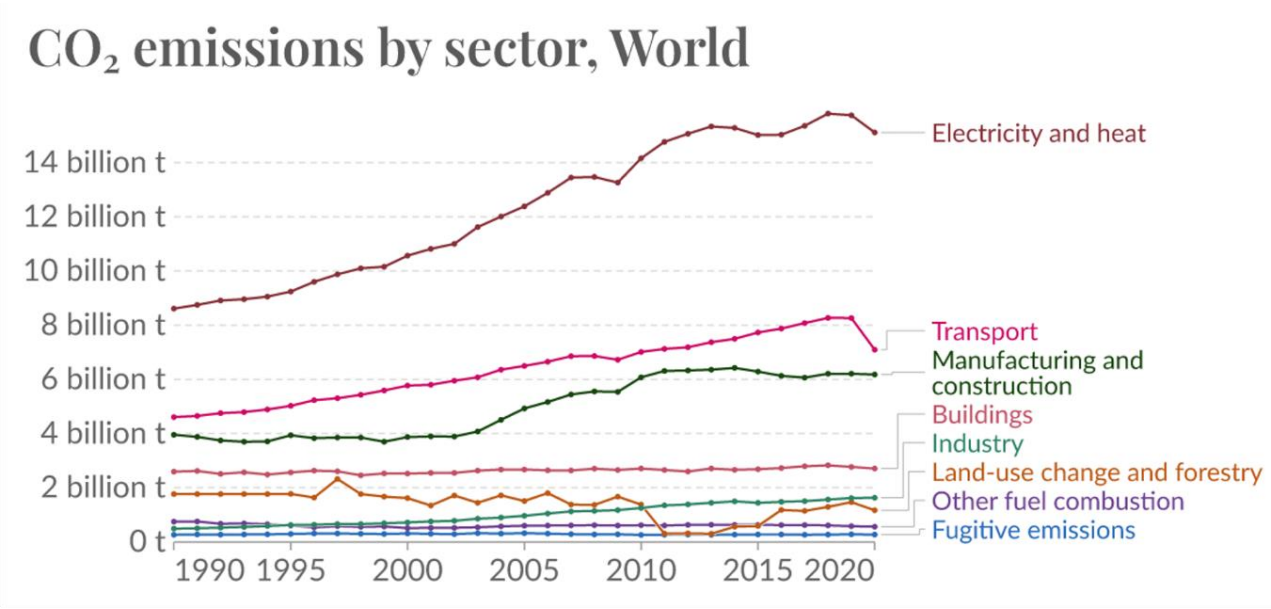

Figure 1.2 Worldwide distribution of CO_2 emissions by different sectors [5].

Therefore, it is important for modern society to switch to green energy carriers that can be produced from sustainable and renewable energy resources (such as the solar, wind, tidal etc.) to fulfil our ever-increasing energy demands [6-9]. Exploring and utilizing clean and renewable energy resources for both the electricity and transportation sectors is a highly effective strategy to decrease carbon emissions and mitigate the impacts on climate change [10]. Thus, shifting towards a CO_2-neutral energy carrier has the potential to greatly reduce CO_2-related emissions. Among various alternatives, hydrogen fuel (H_2) can be used both in electricity and in transportation sectors and offers the highest benefits in terms of low emissions of CO_2 [11].

1.1.1 Hydrogen energy as future fuel

The future era is based on the hydrogen economy. Hydrogen fuel is one of the green energy carriers that can be used as a future energy source for next-generation (**Figure 1.3**) [12]. Currently, up to 96% of the hydrogen used in the world is generated from fossil fuels such as natural gas (48%), crude oil (30%) or coal (18%) through steam reforming, and only about 4% of the hydrogen is produced from water electrolysis [13-14]. Although steam reforming is the most cost-effective method for hydrogen production today, but due to the massive release of CO_2 emissions that should be controlled as the increasing greenhouse effect, this technology is prevented for large production of hydrogen [15-17]. An alternative and environment-friendly method to produce H_2 is to use energy generated by hydropower, wind energy, solar energy, and earth- abundant water as feedstock. Water electrolysis (electrochemical water splitting) is the cleanest way to produce hydrogen and does not cause any adverse effect to the environment. The hydrogen produced by this process is extremely pure (> 99.9%) that is a necessary requirement for the use of hydrogen in fuel cells [18-21]. Hence, hydrogen is often considered a clean energy carrier, because when it is produced from renewable energy sources, it can be used without generating greenhouse emissions.

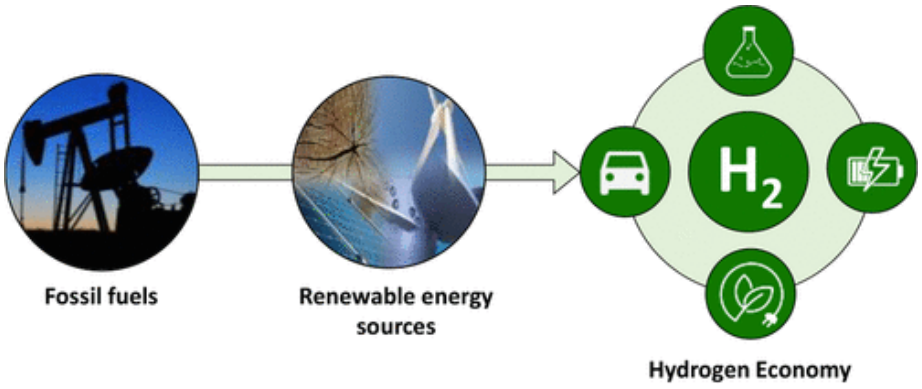

Figure 1.3 Hydrogen production from fossil fuels to renewable sources [12].

1.1.2 Importance of oxygen evolution reaction

Energy conversion from renewable sources is indeed a promising and encouraging solution to reduce our dependence on fossil fuels and address various environmental and energy-related challenges. But then the intermittent nature of such renewable energy sources poses a significant challenge when it comes to their effective utilization [22-24]. Developing high-performance energy conversion and storage (ECS) systems that can efficiently harvest, convert, and store the renewable energy for later use in form of chemical and then reconvert at the point of need, is of great importance, but presents significant scientific and technological challenges. The oxygen evolution reaction (OER) is the core module in these energy conversion and storage (ECS) devices to carry out their reversible process along with oxygen reduction reaction (ORR) and/or hydrogen evolution reaction (HER) [25, 26].

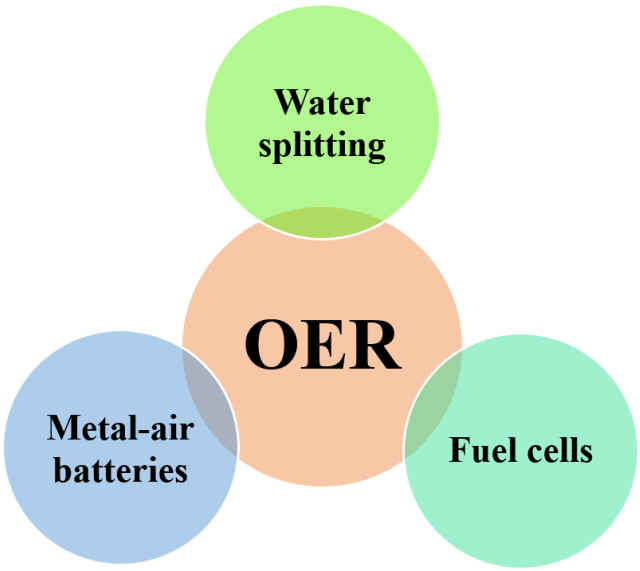

Figure 1.4 Illustrates the importance of OER in different energy systems.

Among the several energy systems driven by electrochemical reactions, the most notable and relevant classifications are: water splitting, metal-air batteries, and fuel cells **(Figure 1.4)** [27-29]. Unfortunately, oxygen electrochemistry plays a critical role in these ECS technologies.

The efficiency of these energy technologies is strongly limited for the oxygen evolution reaction (OER) due to a high overpotential associated with its sluggish kinetics [30-34]. Each of these technologies has unique characteristics and applications, and known for their simplicity, efficiency, and reliability in various context.

1.1.2.1 Water splitting (Electrolysis of water)

Water splitting, also known as water electrolysis, is a chemical process that involves breaking of water molecules (H_2O) into their constituent elements, hydrogen gas (H_2) and oxygen gas (O_2). This process is a key component of various renewable energy and clean hydrogen production technologies. Water splitting typically occurs in an electrolysis cell, which consists of two electrodes (an anode and a cathode) submerged in an electrolytic solution (acidic or alkaline). **Figure 1.5** represents the schematic diagram of a typical water electrolyzer [35]. The electrolyte solution may contain substances like potassium hydroxide (KOH) or sulfuric acid (H_2SO_4) to facilitate the flow of ions. Generally, overall water splitting is based on two half reactions: reduction of H^+ ions at the cathode, i.e., the hydrogen evolution reaction (HER) and oxidation of water at the anode, i.e., the oxygen evolution reaction (OER) [36], as shown below.

$$4H^+ + 4e^- \rightarrow 2H_2,\ E = (0 - 0.059\ pH)V\ vs.\ RHE \quad (1.1)$$

$$2H_2O \rightarrow O_2 + 4H^+ + 4e^-,\ E = (1.23V - 0.059\ pH)\ V\ vs.\ RHE \quad (1.2)$$

$$2H_2O \rightarrow 2H_2 + O_2,\ \Delta E = -1.23V\ vs.\ RHE \quad (1.3)$$

Although, water splitting seems to be an easy and straightforward way to produce H_2, but it is not. The minimum theoretical voltage of 1.23 V is required to drive electrochemical water splitting reaction at room temperature. However, the potential required is commonly much higher at 1.23 V in order to overcome the electrodes' kinetic barrier of the reaction [37, 38]. Water electrolysis is an area where the science and technology need to be improved to overcome the issues associated with it. Yet the production of purest H_2 is the main objective of

water electrolysis, we cannot neglect the counter-reaction (the OER), as it is the sluggish one between them and affects the Faradaic efficiency of the electrolytic cell to a greater extent [39, 40].

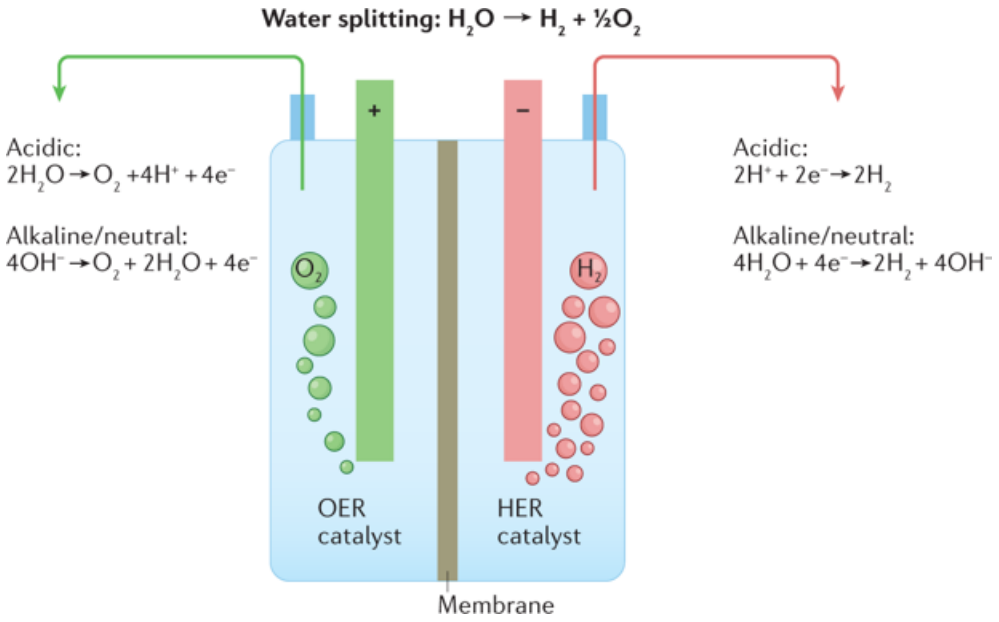

Figure 1.5 Schematic diagram of a typical water electrolyzer [35].

Water oxidation reaction (OER) involves the creation of oxygen-oxygen (O=O) double bond by removing four protons (H^+) from water molecule, which is a crucial step in water splitting. The low activity of water oxidation reaction (OER) at low electrode potential is indeed a significant obstacle in the field of water splitting and this challenge is often referred to as "the low overpotential" problem [39-43]. Researcher, and scientists in the field of electrolysis are actively working to address this challenge and enhance the activity of OER catalysts. To make the water oxidation happen at low potential, several catalysts have been developed. Among them, noble metals occupy the top position due to their better performance [44]. However, their high cost and scarcity hinder their practical applications, therefore recently several attempts have been devoted to break these hurdles by developing inexpensive and earth abundant catalysts [45, 46].

1.1.2.2 Metal-air batteries

Electrochemical energy storage (EES) technologies have immense potential and a wide range of applications, spanning from portable electronic devices to electric vehicles (EVs) and large-scale grid storage. Metal-air battery (MAB) is indeed one of the most promising electrochemical energy storage (EES) systems, mainly due to their high theoretical energy density, eco-friendly nature, good thermal stability, high ionic and electronic conductivity. To date, metal-air batteries have been enormously used in flexible and wearable energy devices [47]. Generally, MABs function in an open system that consists of three basic parts: a metal anode, a porous air cathode, and an electrolyte that separates the two electrodes from one another. **Figure1.6** represents the schematic diagram of the components used in MABs [48].

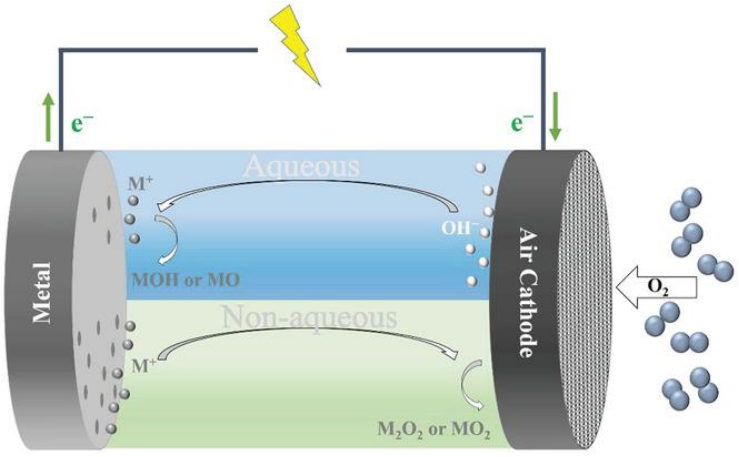

Figure. 1.6 Diagram of metal-air batteries [47].

The low-cost metals such as lithium (Li), sodium (Na), potassium (K), iron (Fe), zinc (Zn), magnesium (Mg), aluminium (Al) can be used as anode material. The utilization of oxygen from ambient air as a cathode source has the additional benefit of lowering the cost and weight of the MABs considerably. The electrolytes used in the MABs can be aqueous, non-aqueous (aprotic), solid-state or hybrid, depending on the nature of the anode employed. Usually, the anodes made of alkali metals (Li, Na, K) are used in non-aqueous electrolytes, due to their extraordinary sensitivity to water. Whereas anodes made of Mg, Al, Fe, or Zn are well-suited

with aqueous electrolytes; these aqueous systems need the addition of a hydrophobic protective layer to prevent electrolyte leakage. This device is basically operating on a fundamental working concept which involves the electrochemical reduction of oxygen from the air at one electrode and the oxidation of metal at another electrode. This leads to the formation of solid metal oxides that may often be recycled or regenerated. This method permits for considerable drop in both the volume and weight of the battery as compared to the traditional Li-ion systems [49-51]. **Figure 1.7** shows the operation of a MAB in aqueous or non-aqueous electrolyte medium. The oxygen behaves differently in an aqueous electrolyte medium from that in a non-aqueous electrolyte, as depicted in **Figure 1.7** [49].

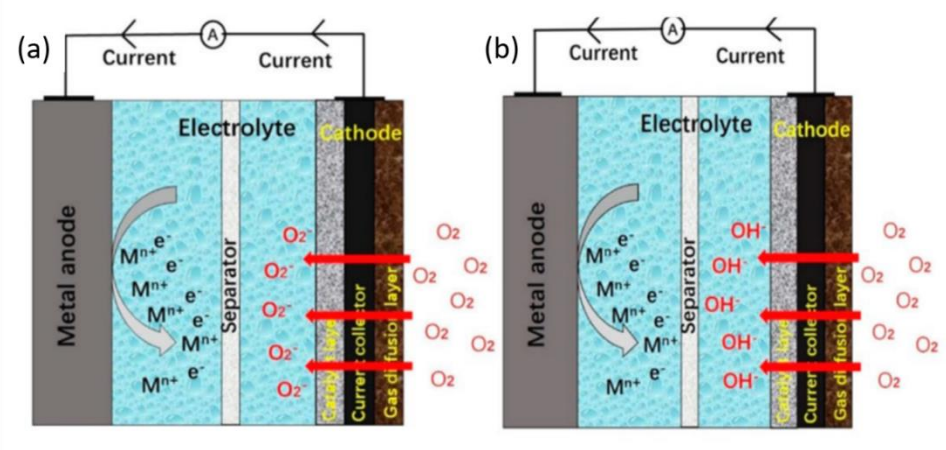

Figure.1.7 Schematic diagrams of MABs working principles for (**a**) non-aqueous electrolyte, and (**b**) aqueous electrolyte [49].

The electrochemical reaction of metal (Zn, Al, Fe, Li) and oxygen in metal-air batteries are described below.

$$\text{Anode: } \mathrm{M} \rightleftharpoons \mathrm{M}^{n+} + n\mathrm{e}^{-} \tag{1.4}$$

$$\text{Cathode: } \mathrm{O_2} + 2\mathrm{H_2O} + 4\mathrm{e}^{-} \rightleftharpoons 4\mathrm{OH}^{-} \tag{1.5}$$

In aqueous electrolyte:

The reaction kinetics of zinc-air batteries (ZABs) in the alkaline aqueous electrolyte is shown below.

$$\text{Anode: } Zn + 4OH^- \rightleftharpoons Zn(OH)_4^{2-} + 2e^- \quad (1.6)$$

$$Zn(OH)_4^{2-} \rightleftharpoons ZnO + 2OH^- + H_2O \quad (1.7)$$

$$\text{Cathode: } \frac{1}{2}O_2 + H_2O + 2e^- \rightleftharpoons 2OH^- \quad (1.8)$$

$$\text{Overall reaction: } \frac{1}{2}O_2 + Zn \rightleftharpoons ZnO \quad (1.9)$$

In non-aqueous electrolyte:

The working principle of Li-air battery (LAB) in the non-aqueous electrolyte is given below.

$$\text{Anode: } 2Li \rightleftharpoons 2Li^+ + 2e^- \quad (1.10)$$

$$\text{Cathode: } O_2 + e^- \rightleftharpoons O_2^- \quad (1.11)$$

$$O_2^- + Li^+ \rightleftharpoons LiO_2 \quad (1.12)$$

$$LiO_2 + Li^+ + e^- \rightleftharpoons Li_2O_2 \quad (1.13)$$

$$\text{Overall reaction: } O_2 + 2Li \rightleftharpoons Li_2O_2 \quad (1.14)$$

Recent reports stated that metal-air batteries performed significantly better compared to metal-ion batteries. MABs exhibit a great advantage regarding theoretical energy density, which is about 3-30 times higher than commercial Li-ion batteries [52]. The theoretical energy density of different types metal-air batteries is shown in **Figure 1.8** [53]. Previous reports suggested that the lithium-air batteries can deliver a theoretical energy density of 11,429 W h kg^{-1} (based on mass of Li metal), which is about 30 times higher compared to commercial Li-ion batteries [52]. However, the current achievable energy density is around 21%, and the power of lithium-air battery is ~0.46 m W g^{-1}, which is only 10% of lithium-ion battery [54, 55].

The development of metal−air batteries has been restricted by problems allied with metal anodes, air catalysts, and electrolytes. Presently, none of them are at a stage for large-scale industrial deployment. Poor cyclic life is another big hurdle for the practical application of metal-air batteries. Their feasibility to replace lithium-ion batteries for future EV applications also remains unclear. Furthermore, these also suffer a poor round-trip efficiency that is ratio of

energy released during discharging to energy required. Nevertheless, the reversible energy process of metal-air batteries is typically controlled by the electrocatalysis of oxygen that depends on the efficiency of catalyst towards ORR and OER reactions [56-58]. The reversibility of metal-air battery mainly depends on the evolution of O_2 from discharge products (M_2O_2 and MO_2, where M represents a metal) and highlights the importance of OER in improving the life span and round-trip energy efficiency for metal-air batteries [59-61]. The OER efficiency strongly depends on the catalytic activity of the cathode catalyst not only to reverse the process but also to keep the air pathway clear for next cycle, by consuming solid products through oxygen evolution [60]. Therefore, boundless efforts have been made to grow new electrocatalysts at low cost that can overtake the state-of-art noble metals, e.g., RuO_2 and IrO_2 [61, 62].

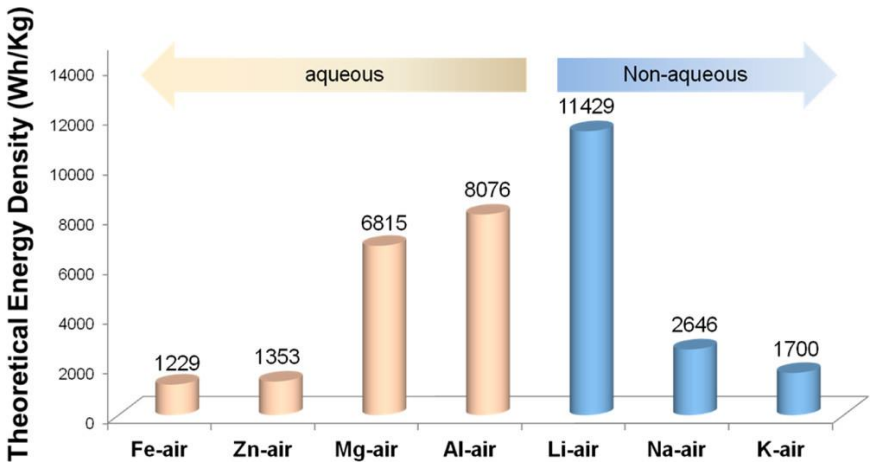

Figure 1.8 Theoretical energy densities for different types of metal− air batteries [52].

1.1.2.3 Fuel cell

Fuel cell is a type of energy conversion device that converts chemical energy to electrical energy by oxidizing the fuel catalysed by the catalysts immobilized on electrodes. Fuel cells offer a cleaner, more efficient, and possibly the most flexible mechanism for energy conversion [63-65]. They have great potential as sustainable power sources for both electric vehicles (EVs) and portable electronics due to their high energy conversion efficiency (generally between 40

to 60% or more), low operation temperature, low or even zero emission, high energy, and power density [66-69]. Generally, a fuel cell is made up of three adjacent components: a fuel electrode (anode), an oxidant electrode (cathode), and an electrolyte sandwiched between them. The electrodes are mainly composed of a porous material that is coated with a layer of catalyst. The molecular hydrogen undergoes an oxidation reaction at the anode, where it generates cations that migrate to the cathode through the electrolyte and free electrons that flow the external circuit. On the other hand, a reduction reaction occurs at the cathode, where oxygen is reduced to water by the cations and electrons [70]. The electrochemical reaction that occurs at the anode and cathode is given below:

$$\text{At anode: } H_2 \rightarrow 2H^+ + 2e^- \tag{1.15}$$

$$\text{At cathode: } 2H^+ + \frac{1}{2}O_2 + 2e^- \rightarrow H_2O \tag{1.16}$$

The overall reaction in the fuel cell produces water (H_2O), heat (Q_{heat}), and electrical work (W_{ele}) as follows:

$$\text{Overall reaction: } H_2 + \frac{1}{2}O_2 \rightarrow H_2O + W_{ele} + Q_{heat} \tag{1.17}$$

There are different kinds of fuel cells, but solid oxide and reversible or regenerative fuel cells (RFCs) get more attention recently, because of their ability of energy storage and fuel resurge, respectively [71, 72]. **Figure1.9** illustrates the basic operational processes within a typical RFC system, which is mainly integrated with an electrolyzer (EL), fuel cell (FC), gas, water, and heat management [71]. The EL and FC modes are the core modules of an RFCs and greatly determine the system performance. During the charging (EL mode), the hydrogen evolution and oxygen evolution reactions (HER and OER) occur at the cathode and anode, respectively. During the discharging (FC mode), the oxygen reduction reaction (ORR) and hydrogen oxidation reaction (HOR) occurs at the cathode and anode, respectively [73, 74]. The electrochemical redox reactions of the EL and FC modes are given below:

(i) EL mode:

$$\text{Anode: } 2H_2O \rightarrow 4H^+ + O_2 + 4e^- \quad (1.18)$$

$$\text{Cathode: } 4H^+ + 4e^- \rightarrow 2H_2 \quad (1.19)$$

$$\text{Overall reaction: } 2H_2O \rightarrow 2H_2 + O_2 \quad (1.20)$$

(ii) FC mode:

$$\text{Anode: } 2H_2 \rightarrow 4H^+ + 4e^- \quad (1.21)$$

$$\text{Cathode: } 4H^+ + O_2 + 4e^- \rightarrow 2H_2O \quad (1.22)$$

$$\text{Overall reaction: } 2H_2O \rightarrow 2H_2 + O_2 \quad (1.23)$$

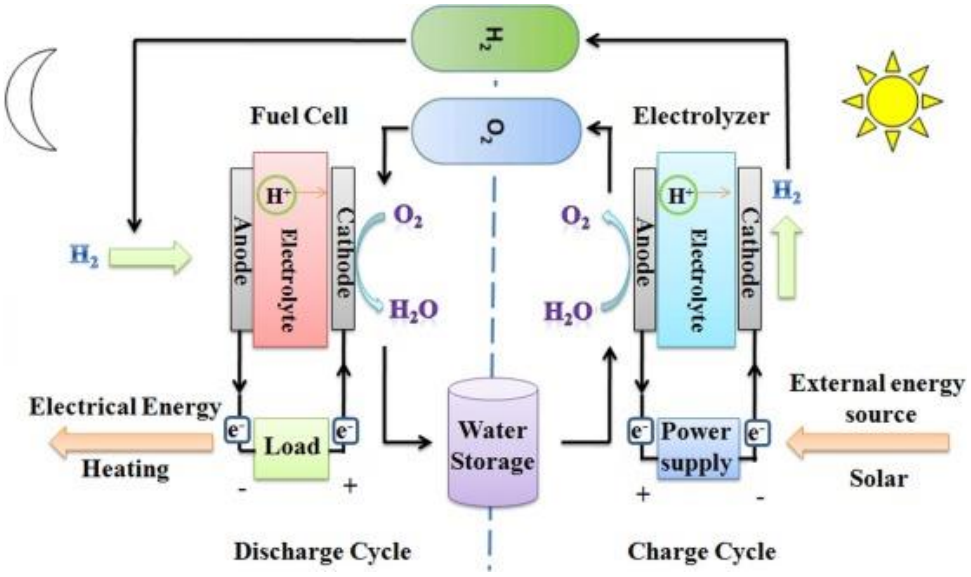

Figure 1.9 Schematic diagram of conventional discrete RFC combined with solar energy sources [71].

RFCs can produce H_2 and O_2 from the waste water during the first cycle through electrocatalysis using electricity. Thus, storing the electrocatalytically produced H_2 can be a key advantage to support the intermittent renewable energy technologies [75-77]. Thus, a regenerative fuel cell which operates in two modes of hydrogen production (electrolyzer cell mode) and power production (fuel cell mode) can provide an economical means for efficient long-term energy storage and on-demand conversion back to electrical energy only with the

participation of powerful oxygen electrolysis. However, the major bottleneck in the market availability of fuel cell is the high-cost of catalyst required for the core reactions involved in both FC and EL modes as well as their poor efficiencies and stabilities. OER is one of the basic chemical reactions in the electrolysis of water to store the energy from its intermittent production systems by fuel cells. But a very little attention has been paid to develop suitable OER catalysts for in-situ electrocatalysis of water in fuel cells. Various state-of-the-art catalysts such as platinum-, ruthenium- or iridium-based materials are commonly used to catalyze these reactions efficiently, but these catalysts cannot meet the large-scale commercialization due to their high-cost and limited reserves. Therefore, the development of inexpensive and earth-abundant material-based catalysts with high catalytic activity and stability are highly desired in both FC and EL technologies [78-80].

1.1.3 Oxygen evolution reaction (OER)

Oxygen evolution reaction is a charge process of generating molecular oxygen (O_2) by a chemical reaction usually from water molecule. The oxygen evolution is one of the most technologically important anodic reactions in electrolytic production of H_2 by water electrolysis [81-83]. Water electrolysis is the simplest and well-known technology for the storage of electricity in the form of non-pollutant hydrogen. The reaction involves the oxidation of H_2O or OH^- to produce O_2 at the anode of an electrolyzer cell. Ideally the reaction proceeds around the thermodynamic limit of 1.23 V versus the reversible hydrogen electrode (RHE) but typically requires large overpotentials of several hundreds of millivolts [84, 85]. The OER is a kinetically sluggish because of their complex electrochemical reaction which proceeds via a multistep, four electron-proton coupled transfer process with variable reaction pathways depending on the pH of the electrolyte and the catalysts used [86]. In an acidic electrolyte, H_2O is oxidized into hydrogen and oxygen, while in alkaline or neutral electrolyte, the hydroxyl ions are oxidized as oxygen and water. The kinetics of the reaction in acidic and alkaline media

are completely dependent on the material by which the reaction is being catalyzed. Noble-metal based catalysts such as Ir and Ru and their compounds catalyze the reaction more efficiently in acidic media. On the contrary, the catalysts based on VIII group 3d transition metals (such as Fe, Co, and Ni and their compounds) catalyze the reaction more favorably in alkaline media. This is mainly correlated to the mechanism by which they catalyze it [87-89]. However, several mechanisms have been proposed for OER in both acidic and alkaline conditions. A detailed review on various reported OER mechanisms in both acidic and alkaline media were summarised by Matsumoto and Sato in 1986 [90], and very recently reiterated by Fabbri et al in 2014 [91], including the Krasil'shchkov [91], Bockris [92], Yeager [93], and Wade and Hackerman [94] pathways together with the most familiar electrochemical oxide pathway and the oxide pathway [95]. In alkaline media, all the anticipated mechanisms instigate with the hydroxide coordination to the active site as an essential elementary step and succeed via other elementary steps. The kinetic barriers accompanied with each elementary step of the reaction mechanism upsurge the overall overpotential required for the OER. An elementary step with the most sluggish kinetics is the rate-determining step (RDS) [89, 91].

❖ **Mechanism of OER in acidic media:**

(i) Electrochemical oxide path [95]

$$S + H_2O \rightarrow S - OH + H^+(aq) + e^- \quad (1.24)$$

$$S - OH \rightarrow S - O^{\cdot} + H^+(aq) + e^- \quad (1.25)$$

$$2S - O^{\cdot} \rightarrow 2S + O_2(g) \quad (1.26)$$

(ii) Oxide path [95]

$$S + H_2O \rightarrow S - OH + H^+(aq) + e^- \quad (1.27)$$

$$2S - OH \rightarrow S - O^{\cdot} + S + H_2O \quad (1.28)$$

$$2S - O^{\cdot} \rightarrow 2S + O_2(g) \quad (1.29)$$

(iii) Krasil'shchkov path [91]

$$S + H_2O \rightarrow S - OH + H^+(aq) + e^- \quad (1.30)$$

$$S - OH \rightarrow S - O^- + H^+(aq) \quad (1.31)$$

$$S - O^- \rightarrow S - O^{\cdot} + e^- \quad (1.32)$$

$$2S - O^{\cdot} \rightarrow 2S + O_2(g) \quad (1.33)$$

(iv) Wade and Hackerman's path [94]

$$2S + 2H_2O \rightarrow S - O^{\cdot} + S - H_2O + 2H^+(aq) + 2e^- \quad (1.34)$$

$$S - O^{\cdot} + 2S - OH^- \rightarrow S - H_2O + 2S + O_2(g) \quad (1.35)$$

❖ **Mechanism of OER in alkaline media:**

(i) Electrochemical oxide path [95]

$$S + OH^-(aq) \rightarrow S - OH + e^- \quad (1.36)$$

$$S - OH + OH^-(aq) \rightarrow S - O^{\cdot} + H_2O + e^- \quad (1.37)$$

$$2S - O^{\cdot} \rightarrow 2S + O_2(g) \quad (1.38)$$

(ii) Oxide path [95]

$$S + OH^-(aq) \rightarrow S - OH + e^- \quad (1.39)$$

$$2S - OH \rightarrow S - O^{\cdot} + S + H_2O \quad (1.40)$$

$$2S - O^{\cdot} \rightarrow 2S + O_2(g) \quad (1.41)$$

(iii) Krasil'shchkov path [91]

$$S + OH^-(aq) \rightarrow S - OH + e^- \quad (1.42)$$

$$S - OH + OH^-(aq) \rightarrow S - O^- + H_2O \quad (1.43)$$

$$S - O^- \rightarrow S - O^{\cdot} + e^- \quad (1.44)$$

$$2S - O^{\cdot} \rightarrow 2S + O_2(g) \quad (1.45)$$

(iv) Yeager's path [92]

$$S + OH^-(aq) \rightarrow S - OH + e^- \quad (1.46)$$

$$S^Z - OH \rightarrow S^{Z+1} - OH + S + e^- \quad (1.47)$$

$$S^{Z+1} - OH + 2OH^{-}(aq) \rightarrow 2S + H_2O + O_2(g) \quad (1.48)$$

(v) Bockris path [93]

$$S + OH^{-}(aq) \rightarrow S - OH + e^{-} \quad (1.49)$$

$$S - OH + OH^{-}(aq) \rightarrow S - H_2O_2 + e^{-} \quad (1.50)$$

$$S - H_2O_2 + OH^{-}(aq) \rightarrow S - O_2H^{-} + H_2O \quad (1.51)$$

$$S - H_2O_2 + S - O_2H^{-} \rightarrow 2S + OH^{-}(aq) + O_2 \quad (1.52)$$

Where, "S" is the surface-active site.

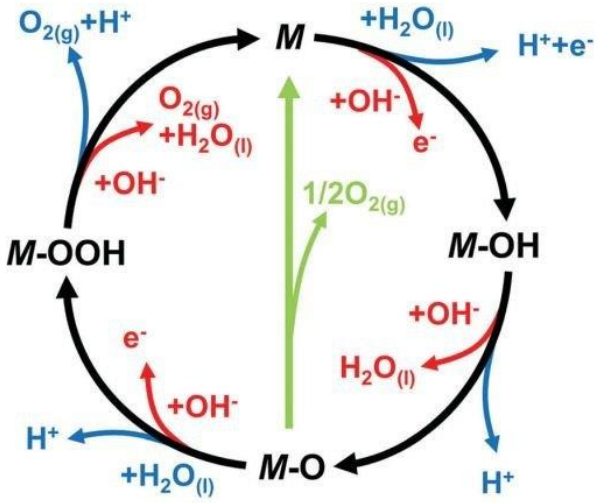

Figure 1.10 The proposed OER mechanism for acid (blue line) and alkaline (red line) conditions. The black line indicates that the oxygen evolution involves the formation of a peroxide (M–OOH) intermediate (black line) while the other route for the direct reaction of two adjacent oxo (M–O) intermediates (green) to produce oxygen is possible as well [96].

The aforementioned-pathways favor the experimental results of both hydroxide and oxide catalysts but shows discrepancies in perovskite materials. To address these discrepancies, many research groups have proposed the electrochemical peroxide path for the O_2 evolution in both the acidic and alkaline conditions. **Figure 1.10** illustrates two possible approaches for OER in both the acidic and alkaline conditions; one is the green route, while other is the black route. Both routes involve the formation of M-O and M-OH intermediates. The green route involves

the direct combination of 2M-O intermediates to release O_2(g) and M directly (here, M is the surface-active site). The other black route (peroxide path) involves the creation of M-OOH intermediate (peroxide) which subsequently decomposes to O_2(g) with the regeneration of the free active sites (M) [96].

However, the major difference in the first elementary steps of all proposed mechanism is the adsorption of water and hydroxide ion on the surface-active site ("S" or "M"). All the proposed mechanism emphasized that the active site ("S" or "M") undergoes a cycle of oxidation and reduction reactions during OER in both acidic and alkaline conditions to evolve O_2 molecules and regenerate the surface sites for the next cycle, as shown in **Figure 1.10**. Thus, metals with variable and stable oxidation states can act as efficient electrocatalysts for OER. Nevertheless, for all the possible OER mechanisms, the formation of intermediates O*, OH* and OOH* on the surface of the electrocatalyst is a prerequisite and behaves as the rate-determining step. This is why Ir and Ru are good electrocatalysts for OER in acidic media and the oxides and hydroxides of Ni, Co, Fe and Mn work better in alkaline conditions [97, 98]. However, it should not be unconsciously believed that all metals which have stable and variable oxidation states can catalyze OER efficiently. The catalytic activity depends on a few other significant characteristics of the catalyst in addition to a favorable electronic configuration and variable oxidation states. One important prerequisite is appropriate bond strength of the intermediates formed in the elementary steps [99, 100]. The bond strength should be neither too strong nor very weak. This is one reason why the oxides and hydroxides of other metals, such as Cu, Os, Re, W, Mo, Cr, V, Ti, and Ta, are either inactive or poorly active materials for OER [101]. The bond strengths of the formed metal–oxygen intermediate species are either too strong or very weak with these metals. Another factor is the stability of the oxides/hydroxides of these metals under two extreme pH conditions.

1.1.4 Factors influencing the performance of OER

The choice of catalyst material is the most influencing factor that governs the kinetics of oxygen evolution reaction (OER). Nevertheless, there are other factors that also affect the reaction kinetics significantly, which are discussed in the following section.

1.1.4.1 Working electrode

The choice of working electrodes/substrates is indeed critical factor in defining the performance of electrochemical systems including the reactions involved in OER. The reaction rate and the overall efficiency of electrocatalytic process are greatly influenced because of their variable structure, conductivity, degree of wettability and access of catalyst to an electrolyte. Depending on the structure and degree of electrolyte mobility, electrode substrates are categorized into two categories: flat surface electrode and 3D electrode. The flat surface electrodes, e.g., glassy carbon (GC), Cu/Ti foil and indium doped tin oxide (ITO) substrate, permit one-way percolation of electrolyte that bounds the catalysis only on surface of catalyst, whereas, the 3D substrates, e.g., carbon cloth/paper (CC and CP) and Ni foam, permit multiple pathways for electrolyte percolation from all sides of catalyst and involve all the material in catalytic reaction. Although all these electrode substrates have their own pros and cons such as, GC electrode is easy to handle and largely used in literature, but suggests a limited mass loading of catalyst (~1 mg cm^{-2}) [102]. Moreover, GC electrode needs a nonconductive binder to stabilize the catalysts, resulting in poor wettability, undesirable and inevitable powder accumulation. These binders can also surge the resistance, block the active sites, and stop diffusion of ions [103]. Consequently, in order to avoid these nonconductive binders, several researchers make efforts to grow catalyst directly on the conductive substrates such as Ni foam, CC (carbon cloth), CP (carbon paper), that leads to strong electrical connection between the catalyst and current collector and brings high gas diffusivity and easy percolation of electrolyte that results in good electrocatalysis.

1.1.4.2 Electrolyte

Different electrolytes (such as alkaline, neutral, or acidic) immensely affect the performance of electrode material. In alkaline media, the OER electrocatalysis is more favourable, while it is very difficult in neutral electrolytes, and come to very low performance in acidic electrolytes. Presently, majority of research is looking for the OER electrocatalysts which are stable in alkaline conditions e.g., carbon-based materials, oxides or oxyhydroxides of transition metals, hybrids, complex ternary (spinel and perovskites). Although, most of these materials are not stable in acidic condition due to high oxidative potential. Thus, an OER electrocatalysts that can work under full range of pH (0–14) is highly desirable [101].

1.1.5 Key performance evaluating parameters for OER

In this section, we will discuss the activity parameters which are widely known for evaluating and comparing the performance of electrocatalysts towards OER.

1.1.5.1 Overpotential (η)

The overpotential (η) is one of the most important parameters for evaluating the performance of OER electrocatalysts. In an ideal case, the reaction proceeds at the potential that will be equal to the reaction potential at equilibrium (i.e., the reversible thermodynamic potential). However, none of the electrochemical reaction proceeds at the potential anticipated only by the thermodynamic considerations diminishing the kinetic barrier practiced in a real system. Because of these kinetic barriers, an additional driving force in terms of an extra potential is required to sustainably drive such electrochemical reactions, which is called the overpotential (denoted by the symbol η). Thus, we can say that the overpotential is the difference between the applied potential (E_{RHE}) and the reversible thermodynamic potential(E_{rev}). The reversible thermodynamic potential (E_{rev}) for OER is 1.23 V vs. the reversible hydrogen electrode

(RHE). Hence, the following equation can be used for OER to calculate the overpotential (η) at a desired current density without iR compensation.

$$\eta_{OER} = E_{RHE} - 1.23\ V \tag{1.53}$$

In general, there are three sources of overpotentials; such as the activation overpotential, the concentration overpotential, and the ohmic or resistance overpotential owing to the uncompensated resistance (Ru), which is exerted by the electrochemical interfaces [91, 101, 104].

- **Activation overpotential:** The activation overpotential (also known as onset overpotential) is an intrinsic property of the catalyst material that catalyzes the electrode reaction and differs from material to material. Hence, it can be reduced by selecting an efficient catalyst.
- **Concentration overpotential:** The concentration overpotential occurs when the electrode reaction begins, there is a rapid drop in concentration at the interfaces due to concentration variance between ions in the bulk of the solution and on the electrode surface. It can be minimized by stirring the electrolyte solution or having a highly concentrated electrolyte.
- **Ohmic or resistance overpotential:** The resistance overpotential can be omitted by performing ohmic drop compensation (also known as *iR*-drop compensation), which is currently accessible in many electrochemical workstations. If not, it can also be done manually by multiplying the resultant current density (i) with uncompensated resistance (Ru), that results in a potential (E). This drop in potential (*iR*-drop), needs to be subtracted from the experimental potential. This means that all studies carried out on new electrocatalytic materials must include data on the overpotential at a defined current density without *iR*-compensation in addition to the *iR*-compensated overpotential at the same defined current density [104-106].

Since, all the proposed mechanisms of the OER proceed via a series of elementary step in both acidic or alkaline media, the kinetic hindrance accompanying with each elementary steps will take part in the overall activation overpotential of an OER catalyst. Man et al. [89] along with other research group [91, 93] have studied the thermodynamics of the OER mechanism and proposed an expression for calculating the theoretical OER overpotential (η_{OER}) under ideal conditions with U = 0 vs. reversible hydrogen electrode (RHE) as follows.

$$\eta_{RHE} = \left(\frac{\Delta G_{max}}{e}\right) - 1.23\ V \tag{1.54}$$

Nevertheless, the theoretical and experimental values had very huge difference in the standard free energy change accompanying with the elementary step of oxide to peroxide conversion. This evidently pronounces that while studying the thermodynamics of the overpotential, the kinetic hindrances are not taken into consideration. The kinetics of these elementary steps is varying from material to material. Thus, instead of the onset overpotential, the overpotential (η_j) at a fixed current density (j) is considered as benchmarking activity parameter to evaluate an electrocatalyst performance for OER [107]. The widely accepted benchmark for current density is 10 mA cm^{-2} for comparing the OER electrocatalyst in different pH conditions. The numerical figure of merit is the current density predicted for 10% competent solar to fuel conversion device, under 1 sun illumination. Materials having an intense redox peak i.e., giving a current density greater than 10 mA cm^{-2} within the potential range of gas evolution and the catalysts showing high performance like layered double hydroxides (i.e., giving current densities more than 500 mA cm^{-2}), the overpotentials at higher current densities such as 50 and 100 mA cm^{-2} are used as alternative activity parameters. Also, the overpotential of a catalyst is mass dependent i.e., it varies with different mass loading [108]. The lower the overpotential value, the better the material's performance towards OER. In general, a catalyst with an overpotential in the 300–400 mV range is regarded as an effective catalyst for OER. The OER

catalysts are classified as ideal (200–300 mV), excellent (300–400 mV), good (400–500 mV), and adequate (beyond 500 mV) as shown in **Figure1.11** [109].

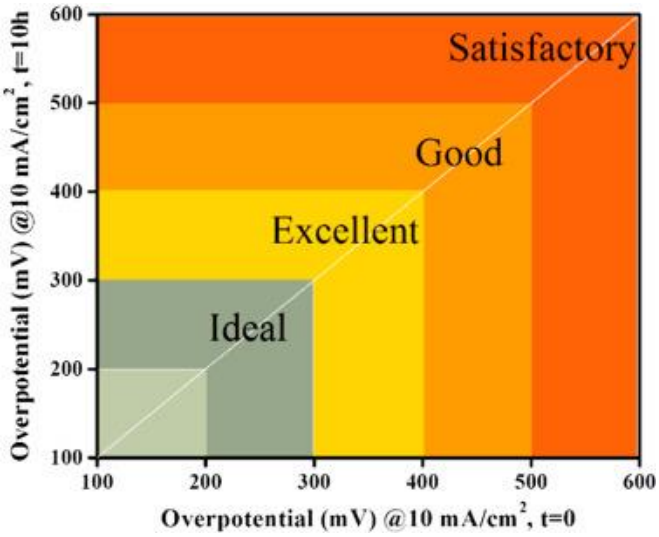

Figure 1.11 The figure of merit for comparison of OER performance of catalysts working in full pH range (acidic to alkaline) [109].

1.1.5.2 Tafel slope and exchange current density

Tafel slope and exchange current density are the two important kinetic parameters of the catalyst performance which gives an insight into the intrinsic kinetic rates of the reaction [110]. In general, the Tafel plot of an electrochemical reaction is obtained by replotting the polarization curves (i.e., Linear sweep voltammogram, LSV) as function of log current density (j) versus overpotential (η). The Tafel equation arise from one of the limiting cases of the Butler-Volmer equation, which gives the relationship between the overpotential and current at the electrical interface. The equation is expressed as follows:

$$j = j_0 \left[exp\left(\alpha_a \frac{nF}{RT} \times \eta\right) - \exp\left(-\alpha_c \frac{nF}{RT} \times \eta\right)\right] \quad (1.55)$$

where j stands for the electrode current density, j_0 is the exchange current density, which represents the current at the equilibrium potential, α_a and α_c refer to the charge transfer

coefficients for anodic reaction (OER) and cathodic reaction (HER), respectively, η is the overpotential, n represents the number of electrons transferred in the reaction (2 in case of HER and 4 in case of OER), F is the Faraday's constant (96,485 C), R is the universal gas constant, and T is the absolute temperature in Kelvin. It is assumed that the applied potential is far away from the equilibrium potential with larger overpotential ($|\eta| \ll RT/nF$) as denoted in eq. 1.55. Thus, for the larger values of positive overpotential, (as in the case for OER), the second term on the RHS of eq. 1.55 becomes zero, and reduces to the following form:

$$j = j_0 exp\left(\alpha \frac{nF}{RT} \times \eta\right) \tag{1.56}$$

It can be rewritten in its logarithmic form, which is also known as the Tafel equation:

$$\ln j = \ln j_0 + \left(\alpha \frac{nF}{RT} \times \eta\right) \tag{1.57}$$

The slope of the linear portion of the Tafel plot is defined as the dependence between the *iR*-compensated overpotential and the current density, which is expressed as follows:

$$\eta = b.\log(j/j_0) \tag{1.58}$$

where b is the Tafel slope given by the formula:

$$\frac{d\log|j|}{d\eta} = \frac{2.303RT}{\alpha\, nF} \tag{1.59}$$

Tafel slope is inversely proportional to the charge transfer coefficient (α), as the remaining other parameters are constants. This specifies that a catalyst with a high charge transfer ability should have a small Tafel slope. The smaller slope value designates that increasing the same current density would need smaller overpotential suggesting a faster reaction rate. This is why it is considered as a primary activity parameter in evaluating the catalytic activity [110-113]. However, this LSV method leads to large error while determining the exchange current density (j_0) when the catalyst is highly capacitive, because exchange current density (j_0) is obtained via the extrapolation of the linear fit which intersects at a point where equilibrium potential (zero potential) of the electrocatalytic process meet the respective current density in logarithmic

scale. In such a case the catalyst with a high overpotential will have a large exchange current density value, which is not possible because a high exchange current density means that transferring electrons across the catalytic interface will be facile and require a very low activation energy. Hence, the result would be a low overpotential [113]. Besides, the electrochemical techniques such as chronoamperometry, chronopotentiometry and electrochemical impedance spectroscopy (EIS) can also be used the extracted Tafel plot with more accuracy [101, 114].

1.1.5.3 Turnover frequency (TOF)

Another kinetic parameter is the turnover frequency (TOF) that is used to determine how quickly a catalyst may catalyze the desired electrochemical reaction at a defined overpotential. It is defined as the number of moles of gas evolved (O_2) at each available catalytic site per unit time and follow pseudo first order kinetics. The following equation is used to calculate the TOFs of any electrocatalytic gas evolution reaction.

$$TOF = \frac{j \times \mathrm{N}_A}{n \times \mathrm{F} \times \Gamma} \tag{1.60}$$

Here, j stands for current density (A cm^{-2}), n is the number of electrons transferred (2 for HER and 4 for OER), N_A is Avogadro number, F is the Faraday constant (96485 C), Γ is the total or surface concentration of active sites of the catalysts or the number of participating atoms in electrocatalyst material. TOF is independent of mass loading but it is highly dependent on the high coverage, i.e., shows linear relationship only if the coverage is below 100%. Higher the TOF value better the catalyst. Several methods are available to determine the surface or total concentration of catalyst in terms of number of atoms. The redox peak in the cyclic voltammogram can be used to find the surface concentration after activation of the catalyst by CV cycling. The total concentration of atoms can be calculated by the Avogadro's number method using the average particle diameter of the catalyst [114-117].

1.1.5.4 Faradaic efficiency

Faradaic efficiency is another quantitative parameter which can be defined as the efficiency of an electrocatalyst to transfer electrons provided by the external circuit across the electrode-electrolyte interface which endorse the electrode reaction i.e., OER and HER. There are two different methods to find the Faradaic efficiency (FE). The first one is the gas chromatography (GC) which is applicable for both OER and HER and the second one is the electrochemical method using a rotating ring disc electrode (RRDE) applicable only for OER. RRDE method is used to determine the FE of an OER electrocatalyst in both acidic and alkaline medium. The setup includes glassy carbon disc and Pt ring/Au disc and Pt ring electrode. The following equation has been used to calculate the FE of an OER electrocatalyst using RRDE.

$$FE = \frac{j_R \times n_D}{j_D \times n_R \times N_{CL}} \tag{1.61}$$

In the above equation, j_R and j_D is the current density at the ring and disc electrode, respectively, n_D is number of electrons transferred at the disc electrode (4 for OER), n_R is number of electrons transferred at the ring electrode for O_2 reduction (4, since the ring electrode is Pt and thus electron pathway probable for ORR on Pt surface) and N_{CL} is collection efficiency of ring electrode. This is very useful method to find the precise activity of an OER catalyst that has the following possibilities of losing its Faradaic efficiency: an OER catalyst with one or more strong redox peaks within the potential window of the OER (almost all Ni-, Co-, and Fe-based catalysts), an electrocatalyst that can facilitate other unwanted side reactions, and an electrocatalyst that heats up during the electrocatalysis process [116-119].

1.1.5.5 Electrochemically active surface area (ECSA)

ECSA is an important parameter for investigating the surface properties of a catalyst. It can be estimated by measuring double-layer capacitance (C_{dl}) using cyclic voltammetry (CV) and impedance spectroscopy (EIS). However, most widely used method to measure the ECSA's of

different catalysts is double layer capacitance (C_{dl}) using cyclic voltammetry (CV). In this method, CV measurements should be performed in a non-faradaic region at various scan rates. The current (i.e., the anodic or cathodic current or the average of the anodic and cathodic current) within the potential window (non-faradaic region) is a charging current (i_c) which exists because of the double layer charging phenomenon and is proportional to the scan rate (ν). The plot of charging current (i_c) against the scan rate (ν) will give a straight line and the slope of this line will give C_{dl} (eq.1.62).

$$i_c = \nu C_{dl} \tag{1.62}$$

The ECSA of a catalyst can be calculated by using the following equation.

$$ECSA = \frac{C_{dl}}{C_s} \tag{1.63}$$

Where, C_s is the specific capacitance of an electrode (metal, nonmetal, and semiconductors). In different electrolytes, the value of C_s is typically varying from 0.015 to 0.130 mF cm^{-2}. Therefore, considering the constant values C_s, it is possible to compare electrocatalysts with their electrochemical double-layer capacitance (C_{dl}), because it has a direct relationship with ECSA. The higher the value of ECSA for catalyst material, the higher will be its OER activity [120, 121].

1.1.5.6 Mass and specific activities

Mass and specific activity are the two another activity parameters that gains much attention for the evaluation of catalyst performance. Both are obtained at a particular overpotential. The overpotential obtained at current density normalized by mass loading of catalyst is specified as mass activity which is expressed as A g^{-1} whereas the overpotential obtained at current density normalized by ECSA or BET is termed as specific activity and expressed as A cm^{-2}. At the present time, geometrical area normalized current density have been used which reflect the area of electrodes with planar and smooth surfaces only. This is not appropriate for electrocatalysts

with uneven or roughened surface area such as in situ grown catalysts or electrodes adapted with nano-powders. N_2 gas adsorption and desorption measurements used in BET (Brunauer–Emmett–Teller) adsorption isotherm determines the real surface area of catalyst, which is not electrochemically active. This method has high chances of having inaccuracies, thus ECSA normalized activity is gaining more attention over BET. Compared to geometrical surface area, ECSA (electrochemically active surface area) is more accurate as they give an insight about the inherent catalytic property of the catalyst. Their disadvantage is that there are number of methods for ECSA determination and the measured values varies from method to method [91, 122].

1.1.5.7 Stability

Stability of an electrocatalyst is an important parameter to evaluate its potential for commercial application. Usually, the stability of catalyst is tested by subjecting it to cyclic voltammetry (CV) cycling at a higher scan rate, (also known as the accelerated degradation test), and to chronoamperometry or chronopotentiometry operating at constant potential or current density. In accelerated degradation test, the number of cycles determines the stability of catalyst material. The number of cycles reported for OER ranges from 250 to 1000. Beyond 1000 cycles, it is rare to see such a report on an OER catalyst with extreme stability. The shift in onset overpotential (η_0) and the overpotential at a defined current density of 10 mA cm^{-2} (η_{10}) are measured as indicative parameters of stability. It is considered that a smaller increase in overpotential (not more than 30 mV) indicates a higher stability of catalyst. Stability under constant exposure to a fixed potential (chronoamperometry) or a fixed current density (chronopotentiometry) is examined for durations of several minutes to hours. A stable current density (e.g., 10 mA cm^{-2} and 50 mA cm^{-2} or 100 mA cm^{-2} in case of high-performance catalysts with strong redox peaks) at their corresponding constant potential for more than 12 h

in chronoamperometric measurements or a negligible increase in the overpotential at a current density of 10 mA cm^{-2} for more than 12 h in chronoamperometric measurements is also another widely recognized parameter for examining the stability of an electrocatalyst [104, 123, 124]. Recently, a set of techniques are also employed to determine the structural and compositional stability of catalyst such as ex-situ and in-situ XRD, XPS, SEM and TEM along with potentiometric studies.

1.2 Literature review

1.2.1 Oxygen evolution electrocatalysts

Since OER is a multistep four-electron transfer process, it involves the formation of different reaction intermediates on the surface of electrocatalyst with the extraction of an electron at each step. This makes the electrocatalyst material in a vital position. To be regarded as an efficient catalyst for oxygen evolution, it must, in fact, overcome challenging obstacles.

- According to the Sabatier principle [126], an appropriate catalyst should bind the reactant (intermediate species) neither too strongly nor too weakly because these conditions result in inadequate reactant adsorption or difficulties removing final products, respectively. The catalyst surface must provide favorable conditions for reaction intermediates to be adsorbed. Hence, catalysts at the top of the Volcano plot are very good electrocatalysts **(Figure 1.12)** [89]. One of the factors contributing to the outstanding activity of the state-of-the-art OER catalysts is their intermediate bonding strength.
- An efficient electrocatalyst must have a greater number of active sites because the electrochemical water oxidation reaction only occurs on active sites that are present at the surface of the catalyst material [127].
- An electrocatalyst must be an electrically good conductor. Because, each intermediate step in the OER process generates an electron that need to be transported via an external circuit to another half part of the water splitting reaction, also known as anode [128].

Therefore, an electrocatalyst that can get beyond these challenges is highly appreciable in the field of electrochemical water splitting.

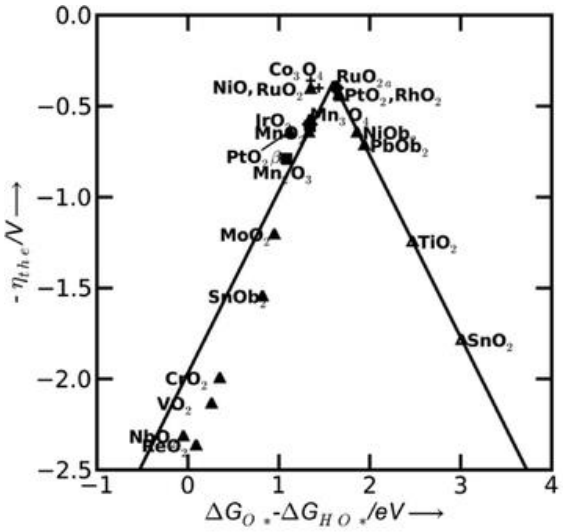

Figure 1.12 Volcano plot presents the theoretical overpotential for oxygen evolution *vs.* the difference between the standard free energy of two subsequent intermediates ($\Delta G^0_{O*} - \Delta G^0_{HO}$) for various binary oxides [89].

1.2.2 Research progress in the field of OER catalysts

In the past decades, considerable efforts have been devoted to the development of an efficient electrocatalyst for OER. To understand the development history of OER catalyst for alkaline water splitting, some key highlights are summarized in **Figure 1.13**.

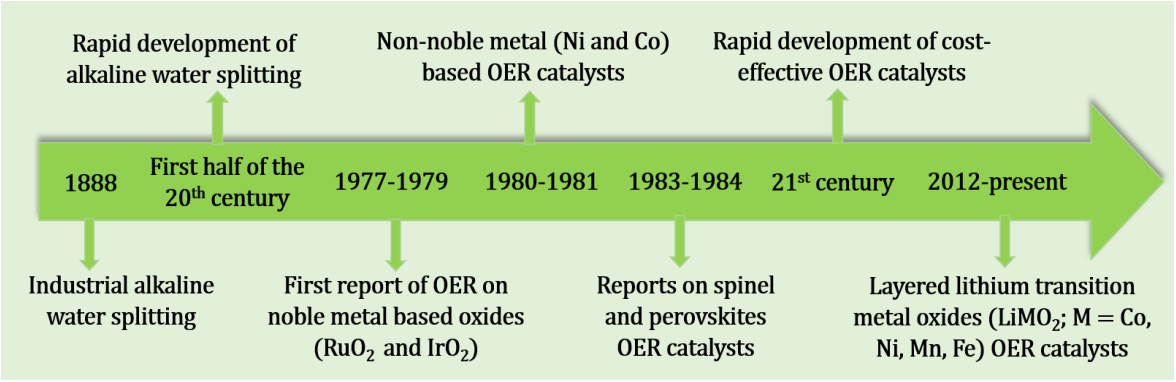

Figure 1.13 Key highlights in the development of OER electrocatalysts.

Luiz Diego Marestoni (1888) developed the industrial method for hydrogen production through alkaline water electrolysis. Afterwards, the rapid development of alkaline water electrolysis technology has been achieved before the first half of the 20th century. The first studies of electrocatalytic OER using RuO_2 and IrO_2 in acid media were reported in 1977 [129] and 1979, respectively [130]. Earlier reports on oxygen evolution catalysts showed that semiconductor oxides (Ni and Co-based oxides) could be used as a material with excellent performance in alkaline electrolytic water [131, 132]. In this section, we discuss about research progress in the field of OER catalysts.

1.2.2.1 Noble-metal based OER electrocatalysts

Noble metals (Ir, Ru, Pd, Pt) and their alloys, oxides and composites are the most studied catalysts due to their excellent performance towards OER. It is experimentally proved that Ir and Ru materials are more active towards OER because of their high stability, low Tafel value and small overpotential as compared to Pt and Pd (Pt < Pd < Ir < Ru) [133-136]. Although Ru exhibits outstanding performance, but its practical applicability is prohibited by its lower stability as compared with the other catalysts. Moreover, Ir and Ru oxides (RuO_2 and IrO_2) are much more active and stable in alkaline media than their pure metal counterparts because pure Ir and Ru are more soluble than oxides in alkaline electrolytes, leading to decreased stability and potential in alkaline electrolytes for commercial scale applications [137]. However, both IrO_2 and RuO_2 are considered as benchmark catalysts for the OER in both acidic [129, 130] and alkaline [137-140] electrolytes. Cherevko *et al*. [141] have demonstrated that IrO_2 is more stable than RuO_2 under OER conditions, but both oxides are unstable at high anodic potentials. The reason behind is that $(Ru^{4+})O_2$ dissolves into the electrolyte in the form of hydrous compound $RuO_2(OH)_2$ and deprotonate into a high oxidation state $(Ru^{8+})O_4$ at high anodic potentials; leading to the deterioration of RuO_2 catalysts. Similarly, $(Ir^{4+})O_2$ also leaches out in the electrolyte by forming $(Ir^{6+})O_3$ at high anodic potentials. However, IrO_2 shows considerably

higher stability but lower OER performance, compared to RuO_2 [142, 143]. One effective strategy to improve the stability of RuO_2 is to mix it with other metals (i.e., Pt [144]) and metal oxides (Ta_2O_5 [145], TiO_2 [146], SnO_2 [147], ZrO_2 [148], and Sb_2O_5 [149]) to form mixed oxides. Several studies have used RuO_2 and IrO_2 mixed oxides, and in combination with other transition metals as OER catalysts. Mamaca *et al.* have shown that doping a small amount of Ir in RuO_2 ($Ru_xIr_{1-x}O_2$) can significantly suppress the deterioration without sacrificing much performance of OER [150]. However, the high cost and low abundance of these noble-metal based oxides is still hinders their large-scale commercialization. As an alternative to address the issue of cost, non-noble metal catalysts need to be explored as OER catalysts for alkaline water electrolysis. Until now, the Ni- and Co-based materials have been intensively investigated as promising non-precious OER electrocatalysts, which are discussed in the next section.

1.2.2.2 Non-noble-metal based OER electrocatalysts

Since noble-metal based OER catalysts are very costly and scarce, there has been momentous interests in oxygen evolution catalysts made of more abundant elements. According to a comprehensive literature review, first row (3*d*) transition metals have been recognized as efficient OER catalysts for decades, because of:

- low cost and high abundance
- high intrinsic activity
- long-term stability under high anodic condition.
- in addition to this, the variable oxidation states, presence of 3*d* electrons and morphological properties of the transition metal compounds make them potentially suitable for use as OER catalysts.
- Modifying the particle sizes, surface areas, and microstructures of these compounds can also improve their performance.

In recent years, noble metals are gradually being replaced by 3*d* transition metal compounds (such as Ni, Co, Mn, Fe, and Cr compounds) which have been thoroughly investigated as OER catalysts. Among them, Ni, and Co based compounds are at the top of the hierarchy of transition metal-based catalyst.

1.2.2.2.1 Ni- and Co-based oxides

Among the transition metal oxide-based catalysts, nickel and cobalt oxides are one of the earlier used oxides as OER catalysts in alkaline medium due to their high stability and special 3*d* electronic configuration. They have been identified as OER catalysts for more than 70 years, and were intensively studied in 1980s. Nickel oxides were first identified as water oxidation catalyst by Bode *et al.* in 1966 [151] and further deep studies were made in the past two decades [152, 153]. Nickel and cobalt oxides are considered as good candidates for the OER because these catalysts are highly resistant to corrosion in alkaline media [99, 154]. In a detailed study of iron-incorporated nickel oxides by Boettcher et al. who revealed that the accidental incorporation of Fe as impurity improved the catalytic activity of NiO_x, Trotochaud et al. (2014) emphasized the significance of Fe impurity effects on catalyst performance [155]. The electrochemical behavior of cobalt metal in alkaline media was first investigated by Wakkad *et al*., and showed that three oxides, namely, CoO, Co_2O_3, and CoO_2, were accessible under anodic bias [156]. Further, the development of alternative structures, such as Co_3O_4, have shown greater prospects [157]. While examine the mechanism of nickel and cobalt oxide electrodes, Lyons *et al.* highlighting the significance of active species (such as Ni^{3+}/Ni^{4+} and Co^{3+}/Co^{4+} redox couple), and putting forth a physisorbed peroxide mechanism that was more broadly applicable [158, 159].

1.2.2.2.2 Spinel oxides

Spinel oxides are another group of compounds, who were studied as promising electrocatalyst for OER, since last century [160, 161]. To date more than 100 compounds in the spinel family

have been reported. The spinel structures contain two octahedral and one tetrahedral coordination in one unit with the general formulation of AB_2O_4, where A and B atoms usually are made up of group 2, group 13 and first-row transition metal elements. They are highly stable with good electrical conductivity in alkaline solution under high anodic potential. Presently, the most widely used electrocatalysts for OER in alkaline medium were Co_3O_4 [162] and $NiCo_2O_4$ [163, 164].

1.2.2.2.3 Perovskites

Perovskites are a large family of oxide materials with the general formula ABO_3, where A is an alkaline-/and or rare earth metal ion, and B is a transition metal ion. The perovskite oxide as OER catalyst was first reported in the 1979 [165]. Since then, several reports have been published revealing that how their properties correlate with electrocatalytic activity. In 1980, Matsumoto *et al*. [166] was the first who established the correlation between bonding properties and catalytic activity. They conducted a detailed study on a $La_{1-x}Sr_xFe_{1-y}Co_yO_3$ system, resulting that the OER activity would increase with increasing amount of x and y. They correlate this result to the band distribution of the d character and the higher oxidation state of the cobalt ion, showing that the OER electrocatalytic activity was closely related to the electrons in the d band of the perovskite. Simultaneously, a very comprehensive and detailed OER investigation based on a perovskite system was also reported by Bockris and Otagawa [167], where they found a trend of OER activity for samples containing different transition metals (Ni > Co > Fe > Mn > Cr). Recently, Shao-Horn and coworkers [168] have published a design approach for high activity perovskite catalyst based on orbital principles and shown that the occupancy of surface transition metal cations in an oxide with the 3*d* electron (e_g symmetry) has a volcano-shaped dependence. A nearly unity e_g occupancy was projected to be the highest OER activity **(Figure 1.14)**.

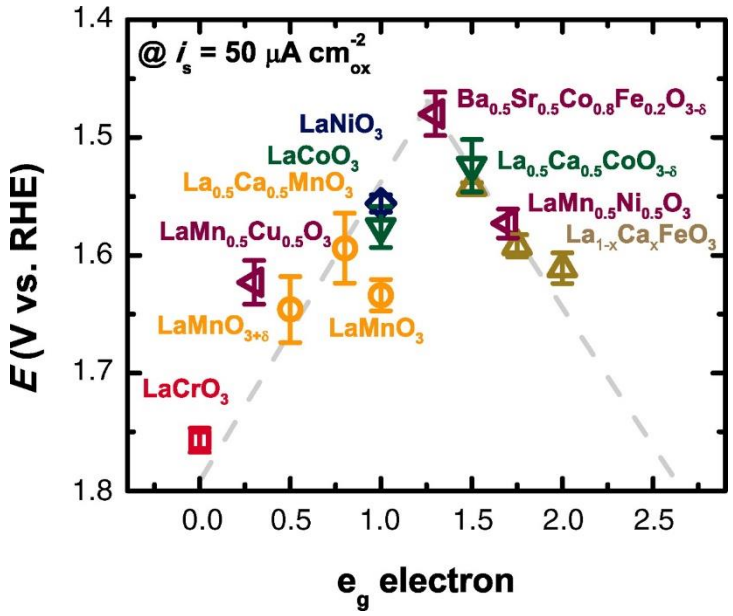

Figure 1.14 The relation between the OER catalytic activity and the occupancy of the e_g-symmetry electron of the transition metal (B in ABO_3) [168].

According to the theory, $Ba_{0.5}Sr_{0.5}Co_{0.8}Fe_{0.2}O_{3-\sigma}$ (BSCF) with e_g occupancy close 1 exhibits the highest efficient activity. Based on this finding, they came to two conclusions regarding how to develop an effective OER catalyst: (1) the e_g electrons should be near to unity, and (2) stronger covalent interaction between transition metal and O atoms was preferable.

1.2.2.2.4 Layered lithium transition-metal oxides (LMOs)

Lithium transition-metal oxides (LMO) with the general formula $LiMO_2$ (M = V, Cr, Co, and Ni), are well known cathode material in lithium-ion batteries. They were come in the existence since 1980s, when layered $LiCoO_2$ was first demonstrated as cathode intercalation material by Goodenough and Mizushima in 1979 [169] and garnered significant interest after the successful commercialization of $LiCoO_2$/carbon-Li-ion technology by Sony in 1991[170]. Nowadays, most of the lithium-ion batteries use $LiCoO_2$. These materials crystallize in the α-$NaFeO_2$ structure with space group R-3m **(Figure 1.15)**. In this structure, O^{2-} ions form a cubic close-packed array, where Li^+ and M^{3+} ions occupy the octahedral interstitial sites on alternating

(111) planes of the rock salt structure and gives an alternating sequence of Li-O-M-O-Li-O-M-O-Li… along the c axis of the unit cell. In Delmas notation [171], this is known as the O3 structure because the metal ions (Li^+ and M^{3+}) occupy the octahedral sites and three MO_2 layers are present per unit cell. M are typically electrochemically active transitional-metal ions, such as manganese, nickel, or cobalt. This layered structure allows fast two-dimensional Li^+ diffusion, assuming there is no cation disorder. The edge-shared MO_6 octahedra provide direct M-M orbital overlap, enabling excellent electronic conductivity.

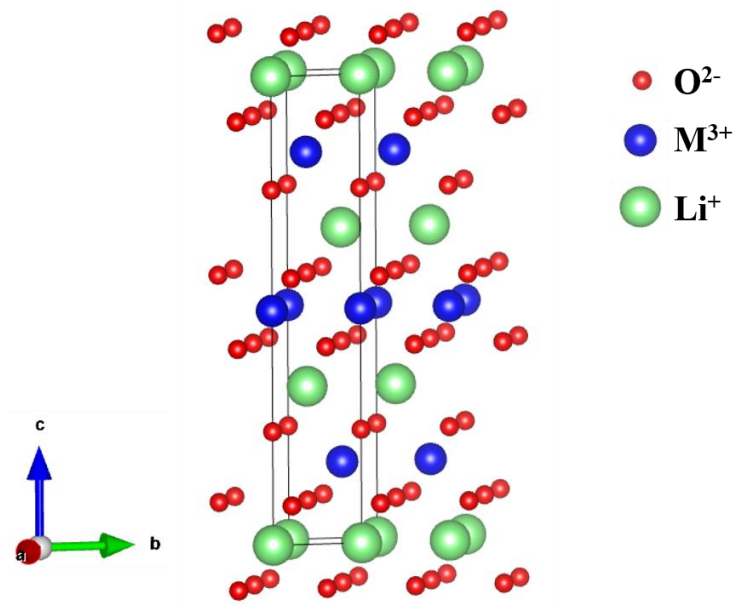

Figure 1.15 Crystal structure of layered $LiMO_2$. [Structure prepared with VESTA Software].

Although these layered oxide cathode materials of Li-ion batteries, in their charged states, are metastable under ambient conditions and at elevated temperature (>200 °C), started to decompose and release O_2 because of the high effective oxygen partial pressure. The evolved oxygen can then react with the organic solvent in the electrolyte and producing heat [172, 173]. The oxygen release from cathode materials remains as one of the key degradation issues of oxygen-containing cathodes. According to Chebiam *et al.* reports, the cathodes $LiCo_{1-x}O_2$ and $LiNi_{1-x}O_2$ of a Li-ion battery have been observed to evolve oxygen at $x > 0.55$ and $x > 0.8$, respectively, which is accompanied by the pinning of the Co^{3+}/Co^{4+} and Ni^{3+}/Ni^{4+} redox

energies at the top of the O-2*p* bands [174, 175], suggesting a strong covalent bonding between the surface oxygen and redox cation, which is required for good OER activity. These findings prompt investigation of $LiMO_2$ cathode materials as potential OER catalysts.

With this motivation, lithium metal oxides (LMOs) are now being explored as OER electrocatalysts due to their notable catalytic activity and following advantages:

- LMOs show a highly concentrated high-activity area with a low overpotential and a fast turn-over efficiency compared to the previously reported OER catalysts, such as commercial IrO_2 and RuO_2, transition metal alloy, hydroxides, and phosphides, **(Figure 1.16a)** [176].
- LMOs have been commercialized for many years due to the rapid growth of lithium-ion batteries, thus LMOs are easy to scale up from either new production or recycled LMOs from battery wastes.
- By varying the lithium content, LMO catalysts can accurately measure the chemical valence of transition metals, and alter their surface structures.

Li-O-M structures have demonstrated distinct physical and chemical characteristics **(Figure 1.16.b)**. A new controlled surface is made possible by the insertion and extraction of lithium ions, which are timed to coincide with the tuning of metal valence in LMOs. This structural reconstruction alters the local electronic structure and reveal the real active centers for the OER. The molecular interactions involved in the oxidation of water are finally tailored by this mechanism. Specifically, the unique layered structure of LMOs can be exfoliated, forming single/few-layer LMO. These properties considerably increase the number of active sites, resulting in an enhanced catalytic activity [177, 178].

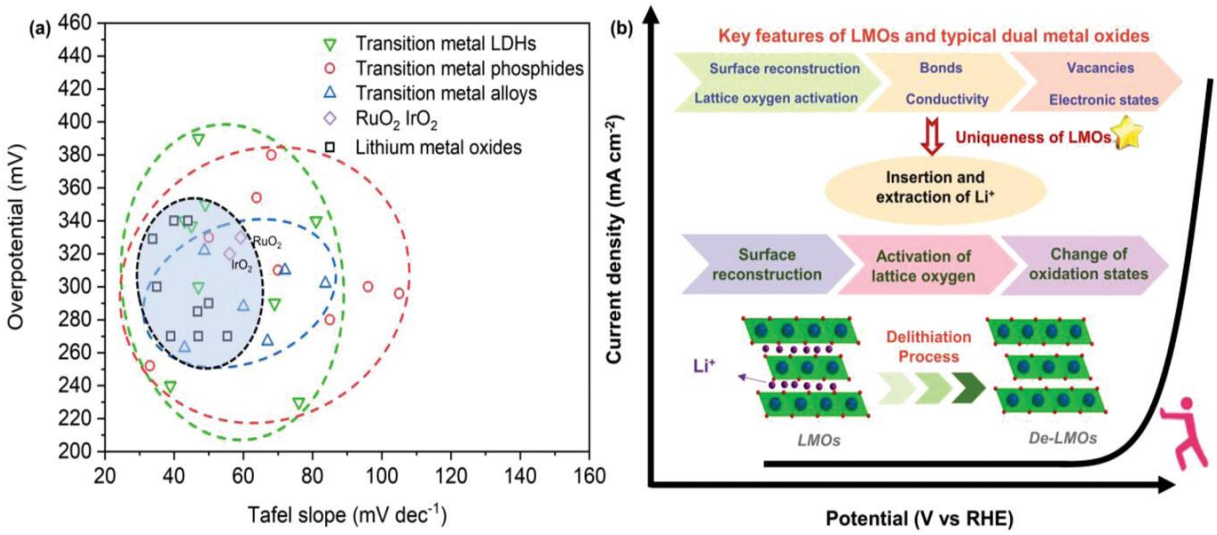

Figure 1.16 (a) Catalytic activity comparison of typical OER catalysts and LMOs in aspects of overpotential and Tafel slope at 10 mA cm^{-2}. **(b)** Key features to understand LMO catalysts [176].

1.2.2.2.4.1 Review on $LiMO_2$ as OER catalysts

In recent years, LMOs have drawn a lot of attention because of their exceptional OER capabilities. Being a typical cathode in lithium-ion batteries, lithium intercalation and extraction allow for the tuning of its electronic structure, making LMOs a highly studied OER catalyst [169, 179]. In 2012, Gardner *et al*. investigated water oxidation catalytic activity of the two polymorphs of lithium cobalt oxides (i.e., $Li_2Co_2O_4$ and $LiCoO_2$) to test the bioinspired hypothesis, and found that $Li_2Co_2O_4$ possesses cubic Co_4O_4 unit in the lattice, which is active in catalyzing the water oxidation reaction, while $LiCoO_2$ consists of alternating layers of Co-O and Li-O octahedra forming $LiCo_3O_4$ units, not cubic Co_4O_4 unit [180]. In 2014, Maiyalagan *et al.* [181] design a low temperature synthesized chemically de-lithiated LT-$Li_{0.5}CoO_2$ catalyst by NO_2BF_4 for the first time, which exhibit a potentially high electrocatalytic activity than that its low temperature-lithiated spinel phase (LT-$LiCoO_2$) and high temperature layered phase (HT-$LiCoO_2$). The high activity of this de-lithiated composition is attributed to the Co_4O_4 cubane subunits and a pinning of the $Co^{3+/4+}$:3d energy with the top of the O^{2-} :2p band **(Figure 1.17)**.

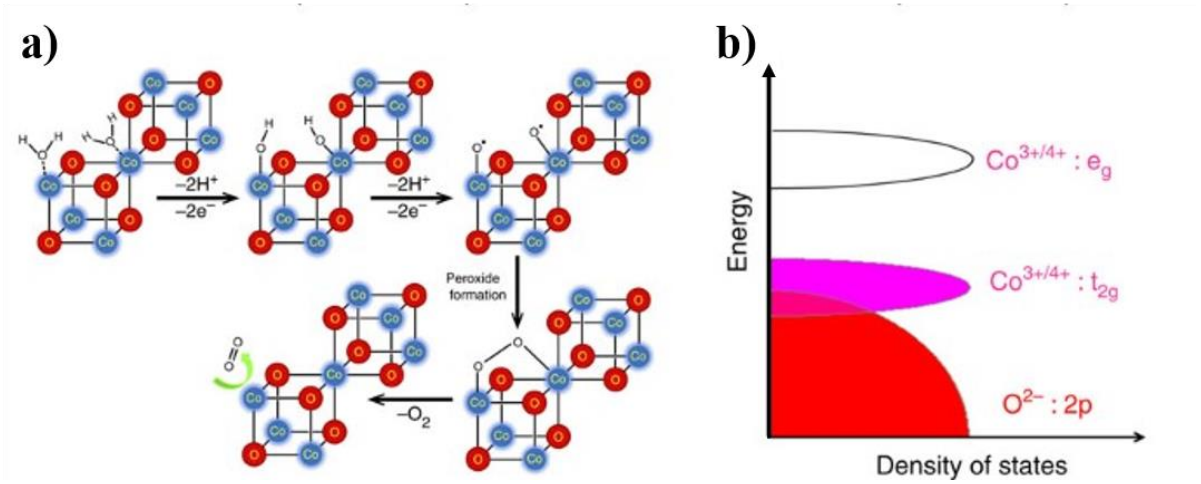

Figure 1.17 (a) Mechanism of OER on Co_4O_4 cubane units in LT-$LiCoO_2$. (b) Qualitative one-electron energy diagram of $Li_{1-x}CoO_2$, illustrating the pinning of the $Co^{3+/4+}$: 3*d* energy with the top of the O^{2-}: 2*p* band [181].

Similarly, Lu *et al.* (2014) [182] performed electrochemical lithiation on $LiCoO_2$ catalyst in organic electrolytes to convert it into $Li_{0.5}CoO_2$ (electrochemical de-lithiated phase) by successively extracting lithium ions from $LiCoO_2$, and tuning the electronic structure of the catalyst. The highly oxidised state of Co ions makes them more hydrophilic to oxygen species, which facilitates their facile binding to OH ions to generate OOH and enhances OER performance. Like $LiCoO_2$, $LiNi_{0.5}Co_{0.2}Mn_{0.3}O_2$ (NCM523) also forms a spinel structure at low temperatures, and its electrochemically de-lithiated state exhibit remarkable OER activity, which is better than the benchmark iridium/carbon catalyst [183]. According to many earlier reports, layered $LiCoO_2$ has a lower catalytic activity than its spinel counterpart and is inert towards OER catalysis. Colligan *et al*. (2015) [184] reported that the LT-$LiCoO_2$ (low temperature spinel form) exhibit better OER performance than HT-$LiCoO_2$ (high temperature layered form), although they share same OER mechanism. The reason behind is because LT-$LiCoO_2$ offers easier surface reconstruction to form the real active centers. Considering this, scientists are still working to prepare layered $LiMO_2$ with high catalytic activity by regulating the morphology, doping, and electrochemical de-lithiation. Recently, Wang et al. carefully

controlled the in-situ catalyst leaching to modify the dynamic surface reorganisation of layered $LiCoO_2$ [185].

In a report, Augustyn *et al.* systematically investigated the behavior of layered $LiMO_2$ oxides ($LiCo_{1-x}Mn_xO_2$, $LiNi_{1-x}Mn_xO_2$, and $LiCo_{1-x}Ni_xO_2$ with $0.25 \leq x \leq 0.7$) for the OER in an alkaline electrolyte. They found that high catalytic activity of Ni- and Co-rich oxides is associated with the low Mn content and the electrochemical surface activation accompanying with the redox of Co and Ni [186]. According to a report, a series of $LiNi_{1-x}Al_xO_2$ with different amount of Al doping were also synthesised by solid-state and solution combustion method and found that the combustion synthesized $LiNi_{0.8}Al_{0.2}O_2$ have shown remarkable OER activity. This technique works well to reduce the mixing of Ni^{2+} in the Li^+ layer, and acquire a high concentration of Ni^{3+}. This thought has been serving as a crucial role to achieve outstanding and stable OER activity [187]. Moreover, $LiNi_{0.5}Co_{0.2}Mn_{0.3}O_2$ (denoted as NCM523) was successfully synthesized into three distinct structures by Huang *et al.* (2020) [188], which are referred as: low temperature synthesized spinel NCM (LT-NCM), high-temperature synthesized lithium-deficient disordered NCM (DO-NCM), and high-temperature layered hexagonal NCM (HT-NCM). Among them DO-NCM displays considerably high OER activity with a low onset potential of 1.48 V vs. RHE. This has been made possible by introducing lithium deficiency in the DO-NCM structure, which can cause the Ni oxidation state to shift from Ni^{2+} to Ni^{3+} by tuning the crystal structure to give more active redox centers, thereby resulting in higher catalytic activity.

1.2.2.2.4.2 Surface chemistry of $LiMO_2$ during the OER

During OER, LMO-based catalysts typically go through structural and chemical changes that are directly related to their durability and activity. The surface chemistry of LMO involved during the OER are as follows **(Figure 1.18)**.

- **Lithium de-intercalation and surface reconstruction**: Lithium-ion de-embedding during OER is a special characteristic of LMO materials. This might change the surface electronic structure by altering the interlayer spacing between surface atoms. Surface reconstruction in conjunction with de-lithiation helps identify the true active sites involved in the OER process [189].
- **Lattice oxygen activation:** With the activation of lattice oxygen, the catalyst surface becomes unstable and changes dynamically during the OER process. The oxidation, exchange, and release of lattice oxygen ligands on the catalyst surface are crucial for OER performance. Lattice oxygen is often activated at two adjacent metal sites, requiring either the catalyst or the lattice oxygen, to exhibit distinct electronic structure [190].
- **Change of metal oxidation states:** The catalyst's oxidation state affects the intrinsic activity of the OER. Higher oxidation states in metal cations result in decreased charge transfer energy due to orbital contraction and valence band shift. The oxidation state of the active metal cation in LMO catalysts can be regulated by doping with other metal elements or de-embedding lithium elements [188].

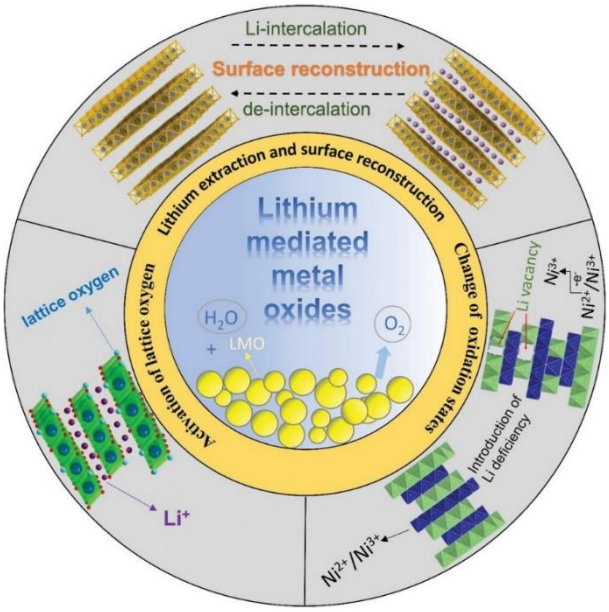

Figure 1.18 Schematic illustration of the chemistry behind changes to the LMO during the OER [176].

1.3 Objective of this work

With an aim to develop highly active electrocatalyst based on earth abundant 3*d* transition metal for oxygen evolution reaction and considering layered $LiMO_2$ (M = Mn, Fe, Co, and Ni) phases, I chose layered $LiCrO_2$ as the material of interest, which is an inactive cathode material in Li-ion battery and not yet studied as an OER electrocatalyst. As priorly discussed, a lot of research has been focused on doping metal oxides with lithium ions to develop efficient catalyst with different active metal sites. The kinetic deficits of the OER can be effectually addressed by the synergistic effects of different metal sites, which include changing the electronic structure and producing more active centers. However, to the best of our knowledge, most of the studies is based on Ni, Co, Mn, and Fe based catalyst and Cr has rarely been investigated as an OER electrocatalyst.

❖ Why $LiCrO_2$?

- crystallize in layered $R\bar{3}m$ structure, like highly active $LiNiO_2$ and $LiCoO_2$ structures, where Li^+ and Cr^{3+} ions occupy the octahedral interstitial sites on alternating (111) planes.
- creating disordering in the structure by introducing partial cation-mixing and Li-vacancy.
- showing irreversible lithium-ion percolation behavior during electrochemical cycle.
- a unique three electron oxidation of Cr^{3+} into Cr^{6+} accompanied by the partial Li-ion extraction.
- not yet explored as OER catalyst.

This thesis tries to offer a unifying idea between electronic structures and electrochemical properties. In this work, I have trying to tune the redox energy of transition metal (3*d*) orbital with respect to the O(2*p*) orbital by introducing foreign metal substituents (Fe, Ni, Al) in

$LiCrO_2$ structure, to access the superior OER catalyst. According to previous research, metal substituents (X^{n+}) with a higher affinity for electrons (i.e., higher electronegativity or stronger Lewis' acid) than the parent metal (M^{n+}) can lower the energy of the antibonding states of M-O bonds by shifting electron density from the parent metal (M) to the ligand (O) through the inductive effect, resulting in a more ionic M-O bond, (as shown in **Figure 1.19**) [191]. This would result in an anodic shift in the redox potential, suggesting a greater overlap between the M(3*d*) and O(2*p*) orbitals, which can often lead to higher OER catalytic activity.

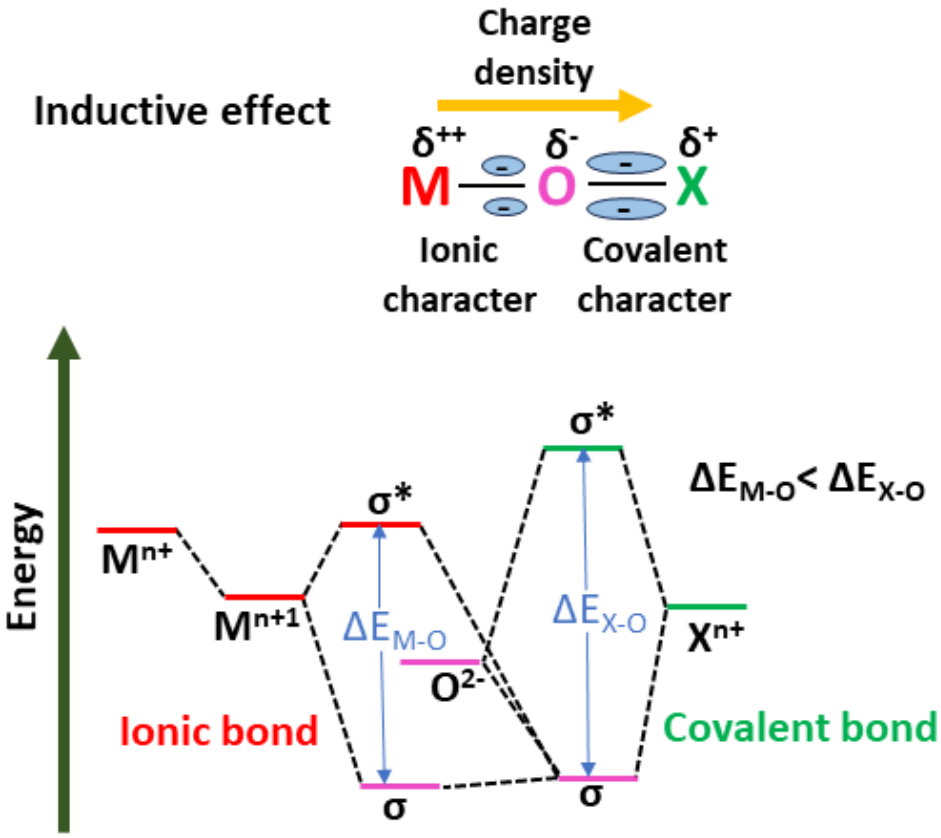

Figure 1.19 Schematic illustration of molecular orbitals of M-O-X presenting the X^{n+} substituted $LiMO_2$, where substituent X^{n+} is more electronegative than M^{n+}. For more electronegative X^{n+}, forming more covalent bond with oxygen than M^{n+}, the energy separation between antibonding and bonding state ($\Delta E_{X\text{-}O}$) is higher than that of M-O bond ($\Delta E_{M\text{-}O}$). By substituting X^{n+}, M-O bond gains more ionic character resulting in a smaller energy separation between bonding and antibonding orbitals ($\Delta E_{M\text{-}O}$).

Encouraged by these findings, I used inductive effect concept for the tuning of redox potential of transition metal ion ($Cr^{3+/6+}$) in $LiCrO_2$ by introducing metal ion substituents (X^{n+} = Fe, Ni, Al) with higher electronegativity or stronger Lewis' acidity in the structure. Doping of highly covalent metal ion (X^{n+}) substituents can effectively increase the ionicity of M-O bond due to the inductive effect, which gives loosely bounded O atom to the active metal ion surface, making O_2 evolution more feasible. The general orbital diagram of X^{n+} substituted $LiMO_2$ is shown in the **Figure 1.19**.

The main objective of this thesis is to design a highly efficient and robust OER catalysts for water splitting through a cost-effective route. In this perspective, this thesis is primarily focused on the following objectives, which are summarized as:

- To synthesize Fe-, Ni- and Al-substituted layered $LiCrO_2$ with different doping concentrations by using solid-state reaction method and solution combustion method.
- To characterize these synthesized materials by several characterization techniques such as XRD, XPS, ICP-MS, SEM, HR-TEM, FTIR, BET etc.

To study the OER activity of the synthesized materials by performing different electrochemical characterizations such as cyclic voltammogram (CV), linear sweep voltammogram (LSV), and electrochemical impedance spectroscopy.

1.4 References

1. Chu, S. and Majumdar, A., 2012. Opportunities and challenges for a sustainable energy future. *nature*, *488*(7411), pp.294-303.
2. Lee, R., 2011. The outlook for population growth. *Science*, *333*(6042), pp.569-573.
3. Cook, T.R., Dogutan, D.K., Reece, S.Y., Surendranath, Y., Teets, T.S. and Nocera, D.G., 2010. Solar energy supply and storage for the legacy and nonlegacy worlds. *Chemical reviews*, *110*(11), pp.6474-6502.
4. Global energy trends: Insights from the 2023 statistical review of world energy.
5. Ritchie, H., Roser, M. and Rosado, P., 2020. CO_2 and greenhouse gas emissions. *Our world in data*.
6. Agbossou, K., Chahine, R., Hamelin, J., Laurencelle, F., Anouar, A., St-Arnaud, J.M. and Bose, T.K., 2001. Renewable energy systems based on hydrogen for remote applications. *Journal of power sources*, *96*(1), pp.168-172.
7. Vosen, S.R. and Keller, J.O., 1999. Hybrid energy storage systems for stand-alone electric power systems: optimization of system performance and cost through control strategies. *International journal of hydrogen energy*, *24*(12), pp.1139-1156.
8. Menzl, F., Wenske, M. and Lehmann, J., 1998. Hydrogen-Production by a Windmill Powered Electrolyser. *HYDROGEN ENERGY PROGRESS*, *1*, pp.757-766.
9. Bose, T.K., Agbossou, K., Benard, P. and St-Arnaud, J.M., 1999. New perspectives on renewable energy systems based on hydrogen.
10. Barthels, H., Brocke, W.A., Bonhoff, K., Groehn, H.G., Heuts, G., Lennartz, M., Mai, H., Mergel, J., Schmid, L. and Ritzenhoff, P., 1998. Phoebus-Jülich: an autonomous energy supply system comprising photovoltaics, electrolytic hydrogen, fuel cell. *International Journal of Hydrogen Energy*, *23*(4), pp.295-301.
11. Turner, J.A., 2004. Sustainable hydrogen production. *Science*, *305*(5686), pp.972-974.
12. Megía, P.J., Vizcaíno, A.J., Calles, J.A. and Carrero, A., 2021. Hydrogen production technologies: From fossil fuels toward renewable sources. A mini review. *Energy & Fuels*, *35*(20), pp.16403-16415.
13. Balat, M., 2008. Potential importance of hydrogen as a future solution to environmental and transportation problems. *International journal of hydrogen energy*, *33*(15), pp.4013-4029.

14. Pilavachi, P.A., Chatzipanagi, A.I. and Spyropoulou, A.I., 2009. Evaluation of hydrogen production methods using the analytic hierarchy process. *International Journal of hydrogen energy*, *34*(13), pp.5294-5303.
15. Turner, J.A., 1999. A realizable renewable energy future. *Science*, *285*(5428), pp.687-689.
16. Turner, J.A., 2004. Sustainable hydrogen production. *Science (New York, NY)*, 305, pp.972-974.
17. Whiteley, K.S., Heggs, T.G., Koch, H., Mawer, R.L., and Immel, W., 2000. Polyolefins. in Ullmann's encyclopedia of industrial chemistry (Wiley). pp. 1-103.
18. Bailera, M., Kezibri, N., Romeo, L.M., Espatolero, S., Lisbona, P. and Bouallou, C., 2017. Future applications of hydrogen production and CO_2 utilization for energy storage: Hybrid Power to Gas-Oxycombustion power plants. *International Journal of Hydrogen Energy*, *42*(19), pp.13625-13632.
19. Sapountzi, F.M., Gracia, J.M., Fredriksson, H.O. and Niemantsverdriet, J.H., 2017. Electrocatalysts for the generation of hydrogen, oxygen and synthesis gas. *Progress in Energy and Combustion Science*, *58*, pp.1-35.
20. Rand, D.A., 2011. A journey on the electrochemical road to sustainability. *Journal of Solid State Electrochemistry*, *15*(7-8), pp.1579-1622.
21. Brauns, J. and Turek, T., 2020. Alkaline water electrolysis powered by renewable energy: A review. *Processes*, *8*(2), p.248.
22. Wang, Z.L., Xu, D., Xu, J.J. and Zhang, X.B., 2014. Oxygen electrocatalysts in metal–air batteries: from aqueous to nonaqueous electrolytes. *Chemical Society Reviews*, *43*(22), pp.7746-7786.
23. Mahmood, N., Tahir, M., Mahmood, A., Zhu, J., Cao, C. and Hou, Y., 2015. Chlorine-doped carbonated cobalt hydroxide for supercapacitors with enormously high pseudocapacitive performance and energy density. *Nano Energy*, *11*, pp.267-276.
24. Tahir, M., Mahmood, N., Zhu, J., Mahmood, A., Butt, F.K., Rizwan, S., Aslam, I., Tanveer, M., Idrees, F., Shakir, I. and Cao, C., 2015. One dimensional graphitic carbon nitrides as effective metal-free oxygen reduction catalysts. *Scientific reports*, *5*(1), p.12389.
25. Gür, T.M., 2018. Review of electrical energy storage technologies, materials and systems: challenges and prospects for large-scale grid storage. *Energy & Environmental Science*, *11*(10), pp.2696-2767.
26. Seh, Z.W., Kibsgaard, J., Dickens, C.F., Chorkendorff, I.B., Nørskov, J.K. and Jaramillo, T.F., 2017. Combining theory and experiment in electrocatalysis: Insights into materials design. *Science*, *355*(6321), p.eaad4998.

27. Huang, Z.F., Song, J., Li, K., Tahir, M., Wang, Y.T., Pan, L., Wang, L., Zhang, X. and Zou, J.J., 2016. Hollow cobalt-based bimetallic sulfide polyhedra for efficient all-pH-value electrochemical and photocatalytic hydrogen evolution. *Journal of the American Chemical Society*, *138*(4), pp.1359-1365.
28. Meng, C., Ling, T., Ma, T.Y., Wang, H., Hu, Z., Zhou, Y., Mao, J., Du, X.W., Jaroniec, M. and Qiao, S.Z., 2017. Atomically and electronically coupled Pt and CoO hybrid nanocatalysts for enhanced electrocatalytic performance. *Advanced Materials*, *29*(9), p.1604607.
29. Lv, Z., Mahmood, N., Tahir, M., Pan, L., Zhang, X. and Zou, J.J., 2016. Fabrication of zero to three dimensional nanostructured molybdenum sulfides and their electrochemical and photocatalytic applications. *Nanoscale*, *8*(43), pp.18250-18269.
30. Walter, M.G., Warren, E.L., McKone, J.R., Boettcher, S.W., Mi, Q., Santori, E.A. and Lewis, N.S., 2010. Solar water splitting cells. *Chemical reviews*, *110*(11), pp.6446-6473.
31. Suen, N.T., Hung, S.F., Quan, Q., Zhang, N., Xu, Y.J. and Chen, H.M., 2017. Electrocatalysis for the oxygen evolution reaction: recent development and future perspectives. *Chemical Society Reviews*, *46*(2), pp.337-365.
32. Ferreira, K.N., Iverson, T.M., Maghlaoui, K., Barber, J. and Iwata, S., 2004. Architecture of the photosynthetic oxygen-evolving center. *Science*, *303*(5665), pp.1831-1838.
33. Kanan, M.W. and Nocera, D.G., 2008. In situ formation of an oxygen-evolving catalyst in neutral water containing phosphate and Co^{2+}. *Science*, *321*(5892), pp.1072-1075.
34. Mallouk, T.E., 2013. Water electrolysis: Divide and conquer, Nat. Chem. 5, pp.362–363.
35. Shih, A.J., Monteiro, M.C., Dattila, F., Pavesi, D., Philips, M., da Silva, A.H., Vos, R.E., Ojha, K., Park, S., van der Heijden, O. and Marcandalli, G., 2022. Water electrolysis. *Nature Reviews Methods Primers*, *2*(1), p.84.
36. Yu, M., Budiyanto, E. and Tüysüz, H., 2022. Principles of water electrolysis and recent progress in cobalt-, nickel-, and iron-based oxides for the oxygen evolution reaction. *Angewandte Chemie International Edition*, *61*(1), p.e202103824.
37. Khan, M.A., Zhao, H., Zou, W., Chen, Z., Cao, W., Fang, J., Xu, J., Zhang, L. and Zhang, J., 2018. Recent progresses in electrocatalysts for water electrolysis. *Electrochemical Energy Reviews*, *1*, pp.483-530.
38. Nuttall, L.J., Fickett, A.P. and Titterington, W.A., 1975. Hydrogen generation by solid polymer electrolyte water electrolysis. *Hydrogen Energy: Part A*, pp.441-455.

39. Grewe, T., Deng, X., Weidenthaler, C., Schüth, F. and Tüysüz, H., 2013. Design of ordered mesoporous composite materials and their electrocatalytic activities for water oxidation. *Chemistry of Materials*, *25*(24), pp.4926-4935.
40. Zha, Y., Disabb-Miller, M.L., Johnson, Z.D., Hickner, M.A. and Tew, G.N., 2012. Metal-cation-based anion exchange membranes. *Journal of the American Chemical Society*, *134*(10), pp.4493-4496.
41. Beainy, A., Karami, N. and Moubayed, N., 2014, November. Simulink model for a PEM electrolyzer based on an equivalent electrical circuit. In *International Conference on Renewable Energies for Developing Countries 2014* (pp. 145-149). Ieee.
42. Wei, C., Rao, R.R., Peng, J., Huang, B., Stephens, I.E., Risch, M., Xu, Z.J. and Shao-Horn, Y., 2019. Recommended practices and benchmark activity for hydrogen and oxygen electrocatalysis in water splitting and fuel cells. *Advanced Materials*, *31*(31), p.1806296.
43. Wang, J., Cui, W., Liu, Q., Xing, Z., Asiri, A.M. and Sun, X., 2016. Recent progress in cobalt-based heterogeneous catalysts for electrochemical water splitting. *Advanced materials*, *28*(2), pp.215-230.
44. Lee, Y., Suntivich, J., May, K.J., Perry, E.E. and Shao-Horn, Y., 2012. Synthesis and activities of rutile IrO_2 and RuO_2 nanoparticles for oxygen evolution in acid and alkaline solutions. *The journal of physical chemistry letters*, *3*(3), pp.399-404.
45. Montoya, J.H., Seitz, L.C., Chakthranont, P., Vojvodic, A., Jaramillo, T.F. and Nørskov, J.K., 2017. Materials for solar fuels and chemicals. *Nature materials*, *16*(1), pp.70-81.
46. Hunter, B.M., Gray, H.B. and Muller, A.M., 2016. Earth-abundant heterogeneous water oxidation catalysts. *Chemical reviews*, *116*(22), pp.14120-14136.
47. Liu, Q., Chang, Z., Li, Z. and Zhang, X., 2018. Flexible metal–air batteries: Progress, challenges, and perspectives. *Small Methods*, *2*(2), p.1700231.
48. Durmus, Y.E., Zhang, H., Baakes, F., Desmaizieres, G., Hayun, H., Yang, L., Kolek, M., Küpers, V., Janek, J., Mandler, D. and Passerini, S., 2020. Side by side battery technologies with lithium-ion based batteries. *Advanced energy materials*, *10*(24), p.2000089.
49. Wang, C., Yu, Y., Niu, J., Liu, Y., Bridges, D., Liu, X., Pooran, J., Zhang, Y. and Hu, A., 2019. Recent progress of metal–air batteries—a mini review. *Applied Sciences*, *9*(14), p.2787.
50. Wang, Y.J., Fang, B., Zhang, D., Li, A., Wilkinson, D.P., Ignaszak, A., Zhang, L. and Zhang, J., 2018. A review of carbon-composited materials as air-electrode bifunctional electrocatalysts for metal–air batteries. *Electrochemical Energy Reviews*, *1*, pp.1-34.

51. Zhang, X.B. ed., 2018. *Metal-Air Batteries: Fundamentals and Applications*. John Wiley & Sons.
52. Wang, H.F. and Xu, Q., 2019. Materials design for rechargeable metal-air batteries. *Matter*, *1*(3), pp.565-595.
53. Li, Y. and Lu, J., 2017. Metal–air batteries: will they be the future electrochemical energy storage device of choice?. *ACS Energy Letters*, *2*(6), pp.1370-1377.
54. Kraytsberg, A. and Ein-Eli, Y., 2011. Review on Li–air batteries—Opportunities, limitations and perspective. *Journal of Power Sources*, *196*(3), pp.886-893.
55. Ma, C., Xu, N., Qiao, J., Jian, S. and Zhang, J., 2016. Facile synthesis of NiCo2O4 nanosphere-carbon nanotubes hybrid as an efficient bifunctional electrocatalyst for rechargeable Zn–air batteries. *International Journal of Hydrogen Energy*, *41*(21), pp.9211-9218.
56. Li, Y. and Dai, H., 2014. Recent advances in zinc–air batteries. *Chemical Society Reviews*, *43*(15), pp.5257-5275.
57. Grande, L., Paillard, E., Hassoun, J., Park, J.B., Lee, Y.J., Sun, Y.K., Passerini, S. and Scrosati, B., 2015. The lithium/air battery: still an emerging system or a practical reality?. *Advanced materials*, *27*(5), pp.784-800.
58. Liu, X., Yuan, Y., Liu, J., Liu, B., Chen, X., Ding, J., Han, X., Deng, Y., Zhong, C. and Hu, W., 2019. Utilizing solar energy to improve the oxygen evolution reaction kinetics in zinc–air battery. *Nature communications*, *10*(1), p.4767.
59. Lu, J., Li, L., Park, J.B., Sun, Y.K., Wu, F. and Amine, K., 2014. Aprotic and aqueous Li–O_2 batteries. *Chemical reviews*, *114*(11), pp.5611-5640.
60. Shao, Y., Ding, F., Xiao, J., Zhang, J., Xu, W., Park, S., Zhang, J.G., Wang, Y. and Liu, J., 2013. Making Li-air batteries rechargeable: Material challenges. *Advanced Functional Materials*, *23*(8), pp.987-1004.
61. Zhang, T., Imanishi, N., Shimonishi, Y., Hirano, A., Takeda, Y., Yamamoto, O. and Sammes, N., 2010. A novel high energy density rechargeable lithium/air battery. *Chemical Communications*, *46*(10), pp.1661-1663.
62. Cheng, F. and Chen, J., 2012. Metal–air batteries: from oxygen reduction electrochemistry to cathode catalysts. *Chemical Society Reviews*, *41*(6), pp.2172-2192.
63. Fan, L., Tu, Z. and Chan, S.H., 2021. Recent development of hydrogen and fuel cell technologies: A review. *Energy Reports*, *7*, pp.8421-8446.
64. Sharaf, O.Z. and Orhan, M.F., 2014. An overview of fuel cell technology: Fundamentals and applications. *Renewable and sustainable energy reviews*, *32*, pp.810-853.

65. Chen, T.W., Anushya, G., Chen, S.M., Kalimuthu, P., Mariyappan, V., Gajendran, P. and Ramachandran, R., 2022. Recent advances in nanoscale based electrocatalysts for metal-air battery, fuel cell and water-splitting applications: An overview. *Materials*, *15*(2), p.458.
66. Ananthachar, V. and Duffy, J.J., 2005. Efficiencies of hydrogen storage systems onboard fuel cell vehicles. *Solar Energy*, *78*(5), pp.687-694.
67. Yoshida, T. and Kojima, K., 2015. Toyota MIRAI fuel cell vehicle and progress toward a future hydrogen society. *The Electrochemical Society Interface*, *24*(2), p.45.
68. Barbir, F., Molter, T. and Dalton, L., 2005. Efficiency and weight trade-off analysis of regenerative fuel cells as energy storage for aerospace applications. *International Journal of Hydrogen Energy*, *30*(4), pp.351-357.
69. Maclay, J.D., Brouwer, J. and Samuelsen, G.S., 2006. Dynamic analyses of regenerative fuel cell power for potential use in renewable residential applications. *International Journal of Hydrogen Energy*, *31*(8), pp.994-1009.
70. Ralph, T.R., Hards, G.A., Keating, J.E., Campbell, S.A., Wilkinson, D.P., Davis, M., St-Pierre, J. and Johnson, M.C., 1997. Low cost electrodes for proton exchange membrane fuel cells: Performance in single cells and Ballard stacks. *Journal of the Electrochemical Society*, *144*(11), p.3845.
71. Pu, Z., Zhang, G., Hassanpour, A., Zheng, D., Wang, S., Liao, S., Chen, Z. and Sun, S., 2021. Regenerative fuel cells: Recent progress, challenges, perspectives, and their applications for space energy system. *Applied Energy*, *283*, p.116376.
72. Qiang, M.Z., 2005. Hydrogen: Green Energy in the 21st Century.
73. Yu, E.H., Wang, X., Krewer, U., Li, L. and Scott, K., 2012. Direct oxidation alkaline fuel cells: from materials to systems. *Energy & Environmental Science*, *5*(2), pp.5668-5680.
74. Sadhasivam, T., Dhanabalan, K., Roh, S.H., Kim, T.H., Park, K.W., Jung, S., Kurkuri, M.D. and Jung, H.Y., 2017. A comprehensive review on unitized regenerative fuel cells: Crucial challenges and developments. *international journal of hydrogen energy*, *42*(7), pp.4415-4433.
75. Shih, Z.Y., Periasamy, A.P., Hsu, P.C. and Chang, H.T., 2013. Synthesis and catalysis of copper sulfide/carbon nanodots for oxygen reduction in direct methanol fuel cells. *Applied Catalysis B: Environmental*, *132*, pp.363-369.
76. Xia, W., Mahmood, A., Liang, Z., Zou, R. and Guo, S., 2016. Earth-abundant nanomaterials for oxygen reduction. *Angewandte Chemie International Edition*, *55*(8), pp.2650-2676.
77. Regmi, Y.N., Peng, X., Fornaciari, J.C., Wei, M., Myers, D.J., Weber, A.Z. and Danilovic, N., 2020. A low temperature unitized regenerative fuel cell realizing 60% round trip

efficiency and 10000 cycles of durability for energy storage applications. *Energy & Environmental Science*, *13*(7), pp.2096-2105.

78. Li, X., Popov, B.N., Kawahara, T., Yanagi, H. 2011. Recent advances in non-precious metal catalyst for oxygen reduction reaction in polymer electrolyte fuel cells. *Energy Environ. Sci.*, 4, pp.114–130.
79. Li, S., Hao, X., Abudula, A. and Guan, G., 2019. Nanostructured Co-based bifunctional electrocatalysts for energy conversion and storage: current status and perspectives. *Journal of Materials Chemistry A*, *7*(32), pp.18674-18707.
80. Zhao, D., Zhuang, Z., Cao, X., Zhang, C., Peng, Q., Chen, C. and Li, Y., 2020. Atomic site electrocatalysts for water splitting, oxygen reduction and selective oxidation. *Chemical Society Reviews*, *49*(7), pp.2215-2264.
81. Ibrahim, H., Ilinca, A. and Perron, J., 2008. Energy storage systems—Characteristics and comparisons. *Renewable and sustainable energy reviews*, *12*(5), pp.1221-1250.
82. Nong, H.N., Falling, L.J., Bergmann, A., Klingenhof, M., Tran, H.P., Spöri, C., Mom, R., Timoshenko, J., Zichittella, G., Knop-Gericke, A. and Piccinin, S., 2020. Key role of chemistry versus bias in electrocatalytic oxygen evolution. *Nature*, *587*(7834), pp.408-413.
83. Seh, Z.W., Kibsgaard, J., Dickens, C.F., Chorkendorff, I.B., Nørskov, J.K. and Jaramillo, T.F., 2017. Combining theory and experiment in electrocatalysis: Insights into materials design. *Science*, *355*(6321), p.eaad4998.
84. Busch, M., Halck, N.B., Kramm, U.I., Siahrostami, S., Krtil, P. and Rossmeisl, J., 2016. Beyond the top of the volcano?–A unified approach to electrocatalytic oxygen reduction and oxygen evolution. *Nano Energy*, *29*, pp.126-135.
85. Shen, P.K., Wang, C.Y., Sun, X. and Zhang, J. eds., 2018. *Electrochemical energy: advanced materials and technologies*. CRC press.
86. Han, L., Dong, S. and Wang, E., 2016. Transition-metal (Co, Ni, and Fe)-based electrocatalysts for the water oxidation reaction. *Advanced materials*, *28*(42), pp.9266-9291.
87. Gong, M. and Dai, H., 2015. A mini review of NiFe-based materials as highly active oxygen evolution reaction electrocatalysts. *Nano Research*, *8*, pp.23-39.
88. Zhang, C., Wang, B., Shen, X., Liu, J., Kong, X., Chuang, S.S., Yang, D., Dong, A. and Peng, Z., 2016. A nitrogen-doped ordered mesoporous carbon/graphene framework as bifunctional electrocatalyst for oxygen reduction and evolution reactions. *Nano Energy*, *30*, pp.503-510.

89. Man, I.C., Su, H.Y., Calle-Vallejo, F., Hansen, H.A., Martínez, J.I., Inoglu, N.G., Kitchin, J., Jaramillo, T.F., Nørskov, J.K. and Rossmeisl, J., 2011. Universality in oxygen evolution electrocatalysis on oxide surfaces. *ChemCatChem*, *3*(7), pp.1159-1165
90. Matsumoto, Y. and Sato, E., 1986. Electrocatalytic properties of transition metal oxides for oxygen evolution reaction. *Materials chemistry and physics*, *14*(5), pp.397-426.
91. Fabbri, E., Habereder, A., Waltar, K., Kötz, R. and Schmidt, T.J., 2014. Developments and perspectives of oxide-based catalysts for the oxygen evolution reaction. *Catalysis Science & Technology*, *4*(11), pp.3800-3821.
92. Hall, D.E., 1983. $Ni(OH)_2$-Impregnated Anodes for Alkaline Water Electrolysis. *Journal of The Electrochemical Society*, *130*(2), p.317.
93. Bockris, J.O.M. and Otagawa, T., 2002. Mechanism of oxygen evolution on perovskites. *The Journal of Physical Chemistry*, *87*(15), pp.2960-2971.
94. Wade, W.H. and Hackerman, N., 1957. Anodic phenomena at an iron electrode. *Transactions of the Faraday Society*, *53*, pp.1636-1647.
95. Bockris, J.O.M., 1956. Kinetics of activation controlled consecutive electrochemical reactions: anodic evolution of oxygen. *The Journal of Chemical Physics*, *24*(4), pp.817-827.
96. Suen, N.T., Hung, S.F., Quan, Q., Zhang, N., Xu, Y.J. and Chen, H.M., 2017. Electrocatalysis for the oxygen evolution reaction: recent development and future perspectives. *Chemical Society Reviews*, *46*(2), pp.337-365.
97. Lyons, M.E. and Burke, L.D., 1987. Mechanism of oxygen reactions at porous oxide electrodes. Part 1.—Oxygen evolution at RuO_2 and $Ru_xSn_{1-x}O_2$ electrodes in alkaline solution under vigorous electrolysis conditions. *Journal of the Chemical Society, Faraday Transactions 1: Physical Chemistry in Condensed Phases*, *83*(2), pp.299-321.
98. Lyons, M.E. and Floquet, S., 2011. Mechanism of oxygen reactions at porous oxide electrodes. Part 2—Oxygen evolution at RuO_2, IrO_2 and $Ir_xRu_{1-x}O_2$ electrodes in aqueous acid and alkaline solution. *Physical Chemistry Chemical Physics*, *13*(12), pp.5314-5335.
99. Subbaraman, R., Tripkovic, D., Chang, K.C., Strmcnik, D., Paulikas, A.P., Hirunsit, P., Chan, M., Greeley, J., Stamenkovic, V. and Markovic, N.M., 2012. Trends in activity for the water electrolyser reactions on 3*d* M (Ni, Co, Fe, Mn) hydr(oxy)oxide catalysts. *Nature materials*, *11*(6), pp.550-557.
100. Subbaraman, R., Tripkovic, D., Strmcnik, D., Chang, K.C., Uchimura, M., Paulikas, A.P., Stamenkovic, V. and Markovic, N.M., 2011. Enhancing hydrogen evolution activity

in water splitting by tailoring Li+-$Ni(OH)_2$-Pt interfaces. *Science*, *334*(6060), pp.1256-1260.

101. Anantharaj, S., Karthick, K. and Kundu, S., 2017. Evolution of layered double hydroxides (LDH) as high-performance water oxidation electrocatalysts: A review with insights on structure, activity and mechanism. *Materials Today Energy*, *6*, pp.1-26.

102. Jiao, Y., Zheng, Y., Jaroniec, M. and Qiao, S.Z., 2015. Design of electrocatalysts for oxygen-and hydrogen-involving energy conversion reactions. *Chemical Society Reviews*, *44*(8), pp.2060-2086.

103. Masa, J., Weide, P., Peeters, D., Sinev, I., Xia, W., Sun, Z., Somsen, C., Muhler, M. and Schuhmann, W., 2016. Amorphous cobalt boride (Co_2B) as a highly efficient nonprecious catalyst for electrochemical water splitting: oxygen and hydrogen evolution. *Advanced Energy Materials*, *6*(6), p.1502313.

104. Anantharaj, S., Ede, S.R., Sakthikumar, K., Karthick, K., Mishra, S. and Kundu, S., 2016. Recent trends and perspectives in electrochemical water splitting with an emphasis on sulfide, selenide, and phosphide catalysts of Fe, Co, and Ni: a review. *Acs Catalysis*, *6*(12), pp.8069-8097.

105. Bard, A.J., Faulkner, L.R. and White, H.S., 2022. *Electrochemical methods: fundamentals and applications*. John Wiley & Sons.

106. Zhu, Y.P., Xu, X., Su, H., Liu, Y.P., Chen, T. and Yuan, Z.Y., 2015. Ultrafine metal phosphide nanocrystals in situ decorated on highly porous heteroatom-doped carbons for active electrocatalytic hydrogen evolution. *ACS Applied Materials & Interfaces*, *7*(51), pp.28369-28376.

107. Gorlin, Y. and Jaramillo, T.F., 2010. A bifunctional nonprecious metal catalyst for oxygen reduction and water oxidation. *Journal of the American Chemical Society*, *132*(39), pp.13612-13614.

108. Gong, M., Li, Y., Wang, H., Liang, Y., Wu, J.Z., Zhou, J., Wang, J., Regier, T., Wei, F. and Dai, H., 2013. An advanced Ni–Fe layered double hydroxide electrocatalyst for water oxidation. *Journal of the American Chemical Society*, *135*(23), pp.8452-8455.

109. Tahir, M., Pan, L., Idrees, F., Zhang, X., Wang, L., Zou, J.J. and Wang, Z.L., 2017. Electrocatalytic oxygen evolution reaction for energy conversion and storage: a comprehensive review. *Nano Energy*, *37*, pp.136-157.

110. Shinagawa, T., Garcia-Esparza, A.T. and Takanabe, K., 2015. Insight on Tafel slopes from a microkinetic analysis of aqueous electrocatalysis for energy conversion. *Scientific reports*, *5*(1), p.13801.

111. Doyle, R.L. and Lyons, M.E., 2016. The oxygen evolution reaction: mechanistic concepts and catalyst design. *Photoelectrochemical Solar Fuel Production: From Basic Principles to Advanced Devices*, pp.41-104.

112. Han, L., Dong, S. and Wang, E., 2016. Transition-metal (Co, Ni, and Fe)-based electrocatalysts for the water oxidation reaction. *Advanced materials*, *28*(42), pp.9266-9291.

113. Anantharaj, S., Kundu, S. and Noda, S., 2021. "The Fe Effect": A review unveiling the critical roles of Fe in enhancing OER activity of Ni and Co based catalysts. *Nano Energy*, *80*, p.105514.

114. Vrubel, H., Moehl, T., Grätzel, M. and Hu, X., 2013. Revealing and accelerating slow electron transport in amorphous molybdenum sulphide particles for hydrogen evolution reaction. *Chemical Communications*, *49*(79), pp.8985-8987.

115. Anantharaj, S., Karthik, P.E. and Kundu, S., 2017. Petal-like hierarchical array of ultrathin Ni $(OH)_2$ nanosheets decorated with Ni $(OH)_2$ nanoburls: a highly efficient OER electrocatalyst. *Catalysis Science & Technology*, *7*(4), pp.882-893.

116. Kumar, T.N., Sivabalan, S., Chandrasekaran, N. and Phani, K.L., 2015. Synergism between polyurethane and polydopamine in the synthesis of Ni–Fe alloy monoliths. *Chemical Communications*, *51*(10), pp.1922-1925.

117. Guo, S.X., Liu, Y., Bond, A.M., Zhang, J., Karthik, P.E., Maheshwaran, I., Kumar, S.S. and Phani, K.L.N., 2014. Facile electrochemical co-deposition of a graphene–cobalt nanocomposite for highly efficient water oxidation in alkaline media: direct detection of underlying electron transfer reactions under catalytic turnover conditions. *Physical Chemistry Chemical Physics*, *16*(35), pp.19035-19045.

118. Guo, S.X., Liu, Y., Bond, A.M., Zhang, J., Karthik, P.E., Maheshwaran, I., Kumar, S.S. and Phani, K.L.N., 2014. Facile electrochemical co-deposition of a graphene–cobalt nanocomposite for highly efficient water oxidation in alkaline media: direct detection of underlying electron transfer reactions under catalytic turnover conditions. *Physical Chemistry Chemical Physics*, *16*(35), pp.19035-19045.

119. Karthik, P.E., Raja, K.A., Kumar, S.S., Phani, K.L.N., Liu, Y., Guo, S.X., Zhang, J. and Bond, A.M., 2015. Electroless deposition of iridium oxide nanoparticles promoted by condensation of $[Ir(OH)_6]_2^-$ on an anodized Au surface: application to electrocatalysis of the oxygen evolution reaction. *RSC Advances*, *5*(5), pp.3196-3199.

120. McCrory, C.C., Jung, S., Peters, J.C. and Jaramillo, T.F., 2013. Benchmarking heterogeneous electrocatalysts for the oxygen evolution reaction. *Journal of the American Chemical Society*, *135*(45), pp.16977-16987.

121. Wei, C., Sun, S., Mandler, D., Wang, X., Qiao, S.Z. and Xu, Z.J., 2019. Approaches for measuring the surface areas of metal oxide electrocatalysts for determining their intrinsic electrocatalytic activity. *Chemical Society Reviews*, *48*(9), pp.2518-2534.

122. Gao, M., Sheng, W., Zhuang, Z., Fang, Q., Gu, S., Jiang, J. and Yan, Y., 2014. Efficient water oxidation using nanostructured α-nickel-hydroxide as an electrocatalyst. *Journal of the American Chemical Society*, *136*(19), pp.7077-7084.

123. Anantharaj, S., Jayachandran, M. and Kundu, S., 2016. Unprotected and interconnected Ru 0 nano-chain networks: advantages of unprotected surfaces in catalysis and electrocatalysis. *Chemical Science*, *7*(5), pp.3188-3205.

124. Zou, X. and Zhang, Y., 2015. Noble metal-free hydrogen evolution catalysts for water splitting. *Chemical Society Reviews*, *44*(15), pp.5148-5180.

125. Liu, K., Zhong, H., Meng, F., Zhang, X., Yan, J. and Jiang, Q., 2017. Recent advances in metal–nitrogen–carbon catalysts for electrochemical water splitting. *Materials Chemistry Frontiers*, *1*(11), pp.2155-2173.

126. Hu, J., Zhang, C., Meng, X., Lin, H., Hu, C., Long, X. and Yang, S., 2017. Hydrogen evolution electrocatalysis with binary-nonmetal transition metal compounds. *Journal of Materials Chemistry A*, *5*(13), pp.5995-6012.

127. Guo, Y., Tang, J., Wang, Z., Sugahara, Y. and Yamauchi, Y., 2018. Hollow porous heterometallic phosphide nanocubes for enhanced electrochemical water splitting. *Small*, *14*(44), p.1802442.

128. Xu, K., Chen, P., Li, X., Tong, Y., Ding, H., Wu, X., Chu, W., Peng, Z., Wu, C. and Xie, Y., 2015. Metallic nickel nitride nanosheets realizing enhanced electrochemical water oxidation. *Journal of the American Chemical Society*, *137*(12), pp.4119-4125.

129. Iwakura, C., Hirao, K. and Tamura, H., 1977. Anodic evolution of oxygen on ruthenium in acidic solutions. *Electrochimica acta*, *22*(4), pp.329-334.

130. Beni, G., Schiavone, L.M., Shay, J.L., Dautremont-Smith, W.C. and Schneider, B.S., 1979. Electrocatalytic oxygen evolution on reactively sputtered electrochromic iridium oxide films. *Nature*, *282*(5736), pp.281-283.

131. Oliva, P., Leonardi, J., Laurent, J.F., Delmas, C., Braconnier, J.J., Figlarz, M., Fievet, F. and De Guibert, A., 1982. Review of the structure and the electrochemistry of nickel hydroxides and oxy-hydroxides. *Journal of Power sources*, *8*(2), pp.229-255.

132. Burke, L.D., Lyons, M.E. and Murphy, O.J., 1982. Formation of hydrous oxide films on cobalt under potential cycling conditions. *Journal of electroanalytical chemistry and interfacial electrochemistry*, *132*, pp.247-261.

133. Reier, T., Oezaslan, M. and Strasser, P., 2012. Electrocatalytic oxygen evolution reaction (OER) on Ru, Ir, and Pt catalysts: a comparative study of nanoparticles and bulk materials. *Acs Catalysis*, *2*(8), pp.1765-1772.

134. Frydendal, R., Paoli, E.A., Knudsen, B.P., Wickman, B., Malacrida, P., Stephens, I.E. and Chorkendorff, I., 2014. Benchmarking the stability of oxygen evolution reaction catalysts: the importance of monitoring mass losses. *ChemElectroChem*, *1*(12), pp.2075-2081.

135. Jiao, Y., Zheng, Y., Jaroniec, M. and Qiao, S.Z., 2015. Design of electrocatalysts for oxygen- and hydrogen-involving energy conversion reactions. *Chemical Society Reviews*, *44*(8), pp.2060-2086.

136. Danilovic, N., Subbaraman, R., Chang, K.C., Chang, S.H., Kang, Y.J., Snyder, J., Paulikas, A.P., Strmcnik, D., Kim, Y.T., Myers, D. and Stamenkovic, V.R., 2014. Activity–stability trends for the oxygen evolution reaction on monometallic oxides in acidic environments. *The journal of physical chemistry letters*, *5*(14), pp.2474-2478.

137. Lee, Y., Suntivich, J., May, K.J., Perry, E.E. and Shao-Horn, Y., 2012. Synthesis and activities of rutile IrO_2 and RuO_2 nanoparticles for oxygen evolution in acid and alkaline solutions. *The journal of physical chemistry letters*, *3*(3), pp.399-404.

138. Pi, Y., Zhang, N., Guo, S., Guo, J. and Huang, X., 2016. Ultrathin laminar Ir superstructure as highly efficient oxygen evolution electrocatalyst in broad pH range. *Nano letters*, *16*(7), pp.4424-4430.

139. Makarova, M.V., Jirkovský, J., Klementová, M., Jirka, I., Macounová, K. and Krtil, P., 2008. The electrocatalytic behavior of $Ru_{0.8}Co_{0.2}O_{2-x}$ —the effect of particle shape and surface composition. *Electrochimica Acta*, *53*(5), pp.2656-2664.

140. Li, H., Tang, Q., He, B. and Yang, P., 2016. Robust electrocatalysts from an alloyed Pt–Ru–M (M= Cr, Fe, Co, Ni, Mo)-decorated Ti mesh for hydrogen evolution by seawater splitting. *Journal of Materials Chemistry A*, *4*(17), pp.6513-6520.

141. Cherevko, S., Geiger, S., Kasian, O., Kulyk, N., Grote, J.P., Savan, A., Shrestha, B.R., Merzlikin, S., Breitbach, B., Ludwig, A. and Mayrhofer, K.J., 2016. Oxygen and hydrogen evolution reactions on Ru, RuO_2, Ir, and IrO_2 thin film electrodes in acidic and alkaline electrolytes: A comparative study on activity and stability. *Catalysis Today*, *262*, pp.170-180.

142. Kötz, R.+., Lewerenz, H.J. and Stucki, S., 1983. XPS studies of oxygen evolution on Ru and RuO_2 anodes. *Journal of The Electrochemical Society*, *130*(4), p.825.

143. Kötz, R.+., Neff, H. and Stucki, S., 1984. Anodic Iridium Oxide Films: XPS-Studies of Oxidation State Changes and O_2 evolution. *Journal of the Electrochemical Society*, *131*(1), p.72.

144. Yao, W., Yang, J., Wang, J. and Nuli, Y., 2007. Chemical deposition of platinum nanoparticles on iridium oxide for oxygen electrode of unitized regenerative fuel cell. *Electrochemistry Communications*, *9*(5), pp.1029-1034.

145. Ardizzone, S., Bianchi, C.L., Cappelletti, G., Ionita, M., Minguzzi, A., Rondinini, S. and Vertova, A., 2006. Composite ternary SnO_2–IrO_2–Ta_2O_5 oxide electrocatalysts. *Journal of Electroanalytical Chemistry*, *589*(1), pp.160-166.

146. Da Silva, L.A., Alves, V.A., Da Silva, M.A.P., Trasatti, S. and Boodts, J.F.C., 1997. Oxygen evolution in acid solution on IrO_2+TiO_2 ceramic films. A study by impedance, voltammetry and SEM. *Electrochimica Acta*, *42*(2), pp.271-281.

147. Balko, E.N. and Nguyen, P.H., 1991. Iridium-tin mixed oxide anode coatings. *Journal of applied electrochemistry*, *21*(8), pp.678-682.

148. Benedetti, A., Riello, P., Battaglin, G., De Battisti, A. and Barbieri, A., 1994. Physicochemical properties of thermally prepared Ti-supported IrO_2+ZrO_2 electrocatalysts. *Journal of Electroanalytical Chemistry*, *376*(1-2), pp.195-202.

149. Chen, G., Chen, X. and Yue, P.L., 2002. Electrochemical Behavior of Novel Ti/IrO_x−Sb_2O_5−SnO_2 Anodes. *The Journal of Physical Chemistry B*, *106*(17), pp.4364-4369.

150. Audichon, T., Mamaca, N., Morais, C., Servat, K., Napporn, T.W., Mayousse, E., Guillet, N. and Kokoh, K.B., 2013. Synthesis of $Ru_xIr_{1-x}O_2$ anode electrocatalysts for proton exchange membrane water electrolysis. *ECS Transactions*, *45*(21), p.47.

151. Bode, H., Dehmelt, K. and Witte, J.J.E.A., 1966. Zur kenntnis der nickelhydroxidelektrode—I. Über das nickel (II)-hydroxidhydrat. *Electrochimica Acta*, *11*(8), pp.1079-1087.

152. Oliva, P., Leonardi, J., Laurent, J.F., Delmas, C., Braconnier, J.J., Figlarz, M., Fievet, F. and De Guibert, A., 1982. Review of the structure and the electrochemistry of nickel hydroxides and oxy-hydroxides. *Journal of Power sources*, *8*(2), pp.229-255.

153. Młynarek, G., Paszkiewicz, M. and Radniecka, A., 1984. The effect of ferric ions on the behaviour of a nickelous hydroxide electrode. *Journal of applied electrochemistry*, *14*(2), pp.145-149.

154. Arciga-Duran, E., Meas, Y., Pérez-Bueno, J.J., Ballesteros, J.C. and Trejo, G., 2018. Effect of oxygen vacancies in electrodeposited NiO towards the oxygen evolution reaction: Role of Ni-Glycine complexes. *Electrochimica Acta*, *268*, pp.49-58.

155. Trotochaud, L., Young, S.L., Ranney, J.K. and Boettcher, S.W., 2014. Nickel–iron oxyhydroxide oxygen-evolution electrocatalysts: the role of intentional and incidental iron incorporation. *Journal of the American Chemical Society*, *136*(18), pp.6744-6753.

156. El Wakkad, S.E.S. and Hickling, A., 1950. The anodic behaviour of metals. Part VI.—Cobalt. *Transactions of the Faraday Society*, *46*, pp.820-824.

157. Dangwal Pandey, A., Jia, C., Schmidt, W., Leoni, M., Schwickardi, M., Schüth, F. and Weidenthaler, C., 2012. Size-controlled synthesis and microstructure investigation of Co_3O_4 nanoparticles for low-temperature CO oxidation. *The Journal of Physical Chemistry C*, *116*(36), pp.19405-19412.

158. Lyons, M.E. and Brandon, M.P., 2008. The oxygen evolution reaction on passive oxide covered transition metal electrodes in aqueous alkaline solution. Part 1-Nickel. *International Journal of Electrochemical Science*, *3*(12), pp.1386-1424.

159. Lyons, M.E. and Brandon, M.P., 2008. The oxygen evolution reaction on passive oxide covered transition metal electrodes in aqueous alkaline solution. Part 1-Nickel. *International Journal of Electrochemical Science*, *3*(12), pp.1386-1424.

160. Rasiyah, P. and Tseung, A.C.C., 1983. A Mechanistic Study of Oxygen Evolution on $NiCo_2O_4$: II. Electrochemical Kinetics. *Journal of the Electrochemical Society*, *130*(12), p.2384.

161. Singh, R.N., Koenig, J.F., Poillerat, G. and Chartier, P., 1990. Electrochemical Studies on Protective Thin Co_3O_4 and $NiCo_2O_4$ Films Prepared on Titanium by Spray Pyrolysis for Oxygen Evolution. *Journal of The Electrochemical Society*, *137*(5), p.1408.

162. Koza, J.A., He, Z., Miller, A.S. and Switzer, J.A., 2012. Electrodeposition of Crystalline Co_3O_4: A Catalyst for the Oxygen Evolution Reaction. *Chemistry of Materials*, *24*(18), pp.3567-3573.

163. Zheng, Z., Geng, W., Wang, Y., Huang, Y. and Qi, T., 2017. $NiCo_2O_4$ nanoflakes supported on titanium suboxide as a highly efficient electrocatalyst towards oxygen evolution reaction. *International Journal of Hydrogen Energy*, *42*(1), pp.119-124.

164. Shao, Y., Zheng, M., Cai, M., He, L. and Xu, C., 2017. Improved electrocatalytic performance of core-shell $NiCo/NiCoO_x$ with amorphous FeOOH for oxygen-evolution reaction. *Electrochimica Acta*, *257*, pp.1-8.

165. Matsumoto, Y., Kurimoto, J. and Sato, E., 1979. Oxygen evolution on $SrFeO_3$ electrode. *Journal of Electroanalytical Chemistry and Interfacial Electrochemistry*, *102*(1), pp.77-83.

166. Matsumoto, Y., Yamada, S., Nishida, T. and Sato, E., 1980. Oxygen evolution on $La_{1-x}Sr_xFe_{1-y}Co_yO_3$ series oxides. *Journal of The Electrochemical Society*, *127*(11), p.2360.

167. Bockris, J.O.M. and Otagawa, T., 1984. The electrocatalysis of oxygen evolution on perovskites. *Journal of The Electrochemical Society*, *131*(2), p.290.

168. Suntivich, J., May, K.J., Gasteiger, H.A., Goodenough, J.B. and Shao-Horn, Y., 2011. A perovskite oxide optimized for oxygen evolution catalysis from molecular orbital principles. *Science*, *334*(6061), pp.1383-1385.

169. Mizushima, K.J.P.C., Jones, P.C., Wiseman, P.J. and Goodenough, J.B., 1980. Li_xCoO_2 ($0< x<-1$): A new cathode material for batteries of high energy density. *Materials Research Bulletin*, *15*(6), pp.783-789.

170. Yoshino, A., Sanechika, K. and Nakajima, T., 1987. *"Secondary Battery," US Patent 4,668,595* (Vol. 26). 1987-05.

171. Mendiboure, A., Delmas, C. and Hagenmuller, P., 1984. New layered structure obtained by electrochemical deintercalation of the metastable $LiCoO_2$ (O_2) variety. *Materials research bulletin*, *19*(10), pp.1383-1392.

172. Dahn, J.R., Fuller, E.W., Obrovac, M. and Von Sacken, U., 1994. Thermal stability of Li_xCoO_2, Li_xNiO_2 and λ-MnO_2 and consequences for the safety of Li-ion cells. *Solid State Ionics*, *69*(3-4), pp.265-270.

173. Jiang, J.R.D.J. and Dahn, J.R., 2004. ARC studies of the thermal stability of three different cathode materials: $LiCoO_2$; $Li[Ni_{0.1}Co_{0.8}Mn_{0.1}]O_2$; and $LiFePO_4$, in $LiPF_6$ and LiBoB EC/DEC electrolytes. *Electrochemistry Communications*, *6*(1), pp.39-43.

174. Chebiam, R.V., Prado, F. and Manthiram, A., 2001. Soft Chemistry Synthesis and Characterization of Layered $Li_{1-x}Ni_{1-y}Co_yO_{2-\delta}$ ($0\leq x\leq 1$ and $0\leq y\leq 1$). *Chemistry of materials*, *13*(9), pp.2951-2957.

175. Chebiam, R.V., Kannan, A.M., Prado, F. and Manthiram, A., 2001. Comparison of the chemical stability of the high energy density cathodes of lithium-ion batteries. *Electrochemistry communications*, *3*(11), pp.624-627.

176. Jiang, S., Suo, H., Zheng, X., Zhang, T., Lei, Y., Wang, Y.X., Lai, W.H. and Wang, G., 2022. Lightest Metal Leads to Big Change: Lithium-Mediated Metal Oxides for Oxygen Evolution Reaction. *Advanced Energy Materials*, *12*(33), p.2201934.

177. Yang, J., Tang, D., Liu, Y., Li, W. and Li, J., 2023. Lithium Electrochemical Tuning Engineering in an Aqueous System of $LiCoO_2$ for Enhanced Oxygen Evolution Activity. *Journal of The Electrochemical Society*, *170*(4), p.046502.

178. Nitta, N., Wu, F., Lee, J.T. and Yushin, G., 2015. Li-ion battery materials: present and future. *Materials today*, *18*(5), pp.252-264.

179. Lu, Z., Jiang, K., Chen, G., Wang, H. and Cui, Y., 2018. Lithium electrochemical tuning for electrocatalysis. *Advanced Materials*, *30*(48), p.1800978.

180. Gardner, G.P., Go, Y.B., Robinson, D.M., Smith, P.F., Hadermann, J., Abakumov, A., Greenblatt, M. and Dismukes, G.C., 2012. Structural requirements in lithium cobalt oxides for the catalytic oxidation of water. *Angewandte Chemie International Edition*, *51*(7), pp.1616-1619.

181. Maiyalagan, T., Jarvis, K.A., Therese, S., Ferreira, P.J. and Manthiram, A., 2014. Spinel-type lithium cobalt oxide as a bifunctional electrocatalyst for the oxygen evolution and oxygen reduction reactions. *Nature communications*, *5*(1), p.3949.

182. Lu, Z., Wang, H., Kong, D., Yan, K., Hsu, P.C., Zheng, G., Yao, H., Liang, Z., Sun, X. and Cui, Y., 2014. Electrochemical tuning of layered lithium transition metal oxides for improvement of oxygen evolution reaction. *Nature communications*, *5*(1), p.4345.

183. Chen, Z., Wang, J., Chao, D., Baikie, T., Bai, L., Chen, S., Zhao, Y., Sum, T.C., Lin, J. and Shen, Z., 2016. Hierarchical porous $LiNi_{1/3}Co_{1/3}Mn_{1/3}O_2$ nano-/micro spherical cathode material: minimized cation mixing and improved Li^+ mobility for enhanced electrochemical performance. *Scientific reports*, *6*(1), p.25771.

184. Colligan, N., Augustyn, V. and Manthiram, A., 2015. Evidence of Localized Lithium Removal in Layered and Lithiated Spinel $Li_{1-x}CoO_2$ ($0 \leq x \leq 0.9$) under Oxygen Evolution Reaction Conditions. *The Journal of Physical Chemistry C*, *119*(5), pp.2335-2340.

185. Wang, J., Kim, S.J., Liu, J., Gao, Y., Choi, S., Han, J., Shin, H., Jo, S., Kim, J., Ciucci, F. and Kim, H., 2021. Redirecting dynamic surface restructuring of a layered transition metal oxide catalyst for superior water oxidation. *Nature Catalysis*, *4*(3), pp.212-222.

186. Augustyn, V. and Manthiram, A., 2015. Characterization of Layered $LiMO_2$ Oxides for the Oxygen Evolution Reaction of Metal–Air Batteries (M = Mn, Co, Ni). *ChemPlusChem*, *80*(2), pp.422-427.

187. Gupta, A., Chemelewski, W.D., Buddie Mullins, C. and Goodenough, J.B., 2015. High-rate oxygen evolution reaction on Al-doped $LiNiO_2$. *Advanced Materials*, *27*(39), pp.6063-6067.

188. Huang, D., Yu, J., Zhang, Z., Engtrakul, C., Burrell, A., Zhou, M., Luo, H. and Tenent, R.C., 2020. Enhancing the electrocatalysis of $LiNi_{0.5}Co_{0.2}Mn_{0.3}O_2$ by introducing lithium deficiency for oxygen evolution reaction. *ACS Applied Materials & Interfaces*, *12*(9), pp.10496-10502.

189. Zheng, X., Chen, Y., Zheng, X., Zhao, G., Rui, K., Li, P., Xu, X., Cheng, Z., Dou, S.X. and Sun, W., 2019. Electronic structure engineering of $LiCoO_2$ toward enhanced oxygen electrocatalysis. *Advanced Energy Materials*, *9*(16), p.1803482.

190. Song, J., Wei, C., Huang, Z.F., Liu, C., Zeng, L., Wang, X. and Xu, Z.J., 2020. A review on fundamentals for designing oxygen evolution electrocatalysts. *Chemical Society Reviews*, *49*(7), pp.2196-2214.

191. Kuznetsov, D.A., Han, B., Yu, Y., Rao, R.R., Hwang, J., Román-Leshkov, Y. and Shao-Horn, Y., 2018. Tuning redox transitions via inductive effect in metal oxides and complexes, and implications in oxygen electrocatalysis. *Joule*, *2*(2), pp.225-244.